CHALMERS
UNIVERSITY OF TECHNOLOGY

Impact of Data from Field Measurements in Numerical Groundwater Modelling

A Case Study in the Kankberg mine, Skellefteå

Master thesis in Infrastructure and environmental engineering

NORA ANDERSSON & NORA PERSSON

DEPARTMENT OF ARCHITECTURE AND CIVIL ENGINEERING

CHALMERS UNIVERSITY OF TECHNOLOGY
Gothenburg, Sweden 2024
www.chalmers.se

Master's thesis 2024

Impact of Data from Field Measurements in Numerical Groundwater Modelling

A Case Study in the Kankberg mine, Skellefteå

NORA ANDERSSON & NORA PERSSON

CHALMERS
UNIVERSITY OF TECHNOLOGY

Department of Architecture and Civil Engineering
Division of Geology and Geotechnics
Engineering geology
Chalmers University of Technology
Gothenburg, Sweden 2024

Impact of data from field measurements in a numerical groundwater model
A Case Study in the Kankberg mine, Skellefteå
NORA ANDERSSON & NORA PERSSON

Supervisor: Johanna Merisalu, Architecture and Civil Engineering, David Wladis, Mark & Miljö HydroSense AB.
Examiner: Lars Rosén, Architecture and Civil Engineering

Master's Thesis 2024
Department of Architecture and Civil Engineering
Division of Geology and Geotechnics
Engineering Geology
Chalmers University of Technology
SE-412 96 Gothenburg

Typeset in LaTeX
Published by Chalmers Open Digital Repository
Gothenburg, Sweden 2024

Impact of Data from Field Measurements in Numerical Groundwater Modelling
A Case Study in the Kankberg mine, Skellefteå
NORA ANDERSSON & NORA PERSSON
Department of Architechture and Civil Engineering
Chalmers University of Technology

Abstract

The purpose of the study was to evaluate the differences in simulated drawdown pattern, area of influence and mine inflow in a numerical groundwater model using different datasets. The modelled object was the possible expansion Kankberg mine. Simulations were made in three models calibrated to open-source data and field measurements of different quality respectively. The field measurements were used to calibrate the structures of the Kankberg mining system. From the calibrated models, the expansion was added, and results were obtained.

It was found that the lower quality data, i.e. the open-source data, was not sufficient to model a correct representation of the current mine. Predictions of mine inflow, drawdown and area of influence with the expansion were considered underestimated. Adding next level of data quality resulted in better predictions of area of influence and drawdown but underestimations in inflow. Similar results were found for the model containing the highest quality of data, which on the other hand was considered under-calibrated.

From the study, it was concluded that groundwater level measurements were the most valuable field measurement in groundwater numerical modelling. Measured inflow was considered the second most valuable parameter followed by evaluated hydraulic conductivity. The recommendation suggests a focus on measuring groundwater levels and inflow in the exploration drift when conducting a representative numerical groundwater model in the environmental permit application process for mine construction.

Keywords: numerical groundwater modelling, hydrogeology, MODFLOW-NWT, crystalline bedrock, data value.

Acknowledgements

First and foremost, we would like to express our deep appreciation for our supervisors Johanna Merisalu, doctoral student at the Division of Geology and Geotechnics at Chalmers and David Wladis at Mark & Miljö Hydrosense AB. A big thank you to Johanna Merisalu for providing us with excellent supervision and support in the report writing and geological conceptualisation, it has been very valuable for the thesis. Also, we would like to give a big thanks to David Wladis for sharing his expertise on modelling in bedrock and giving us valuable insights for our professional life. We are also grateful to Sofie Axéen for providing support in the modelling in Python. Also, special thanks for Lars Rosén for providing us feedback on the project, helping us perfecting it. Lastly, we would like to acknowledge Jenny Palmenäs at BergAB for creating the project.

Nora Andersson & Nora Persson, Gothenburg, June 2024

Contents

List of Figures

List of Tables

1
Introduction

Resource extraction within the mining industry is crucial for upholding the standard of life in a modern society (Moran et al., 2014). The global demand on metals and minerals are expected to increase, putting pressure on mining activity to develop the extraction. Mining operations are historically associated with societal and environmental impacts in many places in the world. Some consequences of mining activity have been, to mention a few, displacement of indigenous communities, contamination of water, land and air, and large generation of waste. Additional consequences could include biodiversity loss, water consumption, great energy consumption and impaired health due to the working environment (Aramendia et al., 2023). However, with consideration for the local communities and thoughtful operations, mining could provide valuable socioeconomic benefits to a region (Söderholm and Svahn, 2015). The sustainability of mining activity is therefore a relevant challenge from both an economic, and a societal and ecological point of view.

The mining industry in Sweden has historically been a large contributor to the economic development in the country. In a recent investigating report from Swedish Government Official Reports, the Swedish government state that metals like iron and copper are important for the green transition (SOU, 2022). Although, several issues have been identified with current mining operations and the possible exploitation's of new ones. These issues are related both to social and ecological sustainability were finding the common interest with local residents and protecting nature are central topics. The environmental incidents caused by mining activity are often related to water (Wessman et al., 2014). Issues regarding water is regulated by EU environmental laws and policies, which includes water management regarding both surface water and groundwater (SOU, 2022).

Mining operations are associated with affecting the groundwater both in terms of quality and quantity (Jain et al., 2016). The quality of the groundwater can be impacted by on-site waste, but also due to leaching of pollutants (SOU, 2022). Consequences of this can relate to impaired chemical and ecological status of nearby surface water bodies and watersheds according to the EU policies. In terms of groundwater quantity, the largest impact can be related to dewatering of leaking groundwater into the mine (Jain et al., 2016). Dewatering is not only used in the field of mining, but also as a common measure in large underground construction projects (Pujades and Jurado, 2021). The groundwater that naturally flows into the mine is continuously pumped and removed to ensure a dry working environment. Problems emerging with pumping are related to lowering of groundwater levels in the

surrounding aquifers. A lowered water table can have an impact on both recharge and groundwater flow within the watershed (Jain et al., 2016). Aquifers and local watersheds are important for vegetation and wildlife, as well as for human drinking water supply. Lack of proper water management in the planning stage of a mine is therefore of interest for both local communities, economic actors and to protect the environment (Wessman et al., 2014).

The expected impact on groundwater is an important part of retrieving a permit for the mining operations from the Swedish Land and Environmental Court (SGU, 2016). The impact can be assessed with monitoring of groundwater levels, conducting pumping tests but also by simulations in numerical models. The aim of modelling is to estimate the future variation in groundwater levels (Jain et al., 2016). In the permit application, the effect of the mining operations needs to be described by for e.g., using the predictions retrieved from modelling and monitoring (SGU, 2016).

The investigations that are included in the permit application can have quite a large range in cost both in terms of field measurements and fulfillment, depending on the type and scale. The content of the application will result in decisions for what types of requirements that will be set in the legal permit by the Swedish Land and Environmental Court (Michanek and Zetterberg, 2017). The requirements are therefore a direct result of the quality and accuracy of the presented field assessment. If the quality of the field assessment is low, requirements can be set unreasonably for the site causing large cost of fulfillment in the operational stage. Fulfilling the requirements are crucial to not violate the environmental permit and face consequences such as fines and additional costs for applying for a new permit. A financial balance could therefore be considered between the gathering of sufficient material for reasonable compliance costs to the potential costs and risks of violating the permit.

The Kankberg mine is located outside of Skellefteå in the northern parts of Sweden and is operated by the company Boliden Minerals AB. Several metals have been extracted at the site since 2012 including gold, silver, and tellurium according to the annual summary report from 2021 (Voigt and Bradley, 2020). The mine is currently operated as an underground mine between levels -320m to -530m, through cut and fill methods. The underground mine is reached from a previous open pit mine which started operations in 1966 at +275m which now is called “The Old Kankberg Mine”. The site has potential for an expansion, and the environmental permit is currently drafted for depths between -50m to -300 as well as -600m to -1000m according to Voigt and Bradley (2020).

1.1 Aim

The aim of the project is to evaluate the impact of site-specific data from field measurement on the reliability of results from a numerical groundwater model. The aim is reached by comparing several models ability to forecast the groundwater drawdown patterns, the area of influence and mine inflow when inducing stress from

Kankberg mine in the model. The differences between the models' constitutes of the different level of detail of input data.

1.1.1 Research questions & objectives

Specifications of the issue and the project tasks are presented as research questions and objectives below. The questions and objectives aim to describe the tasks and the intended outcome of the project.

Research questions:

- What is the impact of using field measurements in a numerical groundwater model compared to only using open-source data, considering model accuracy?
- Which type of data is the most valuable to retrieve reliable results for groundwater drawdown and draining patterns with numerical modelling?
- What quality of data is needed for a reliable assessment in the permit process?

Objectives:

- Compare and evaluate groundwater drawdown patterns, the area of influence and mine inflow from a numerical groundwater model using only open-source data, to a numerical groundwater model calibrated with field measurements from two datasets.
- Constitute a recommendation on what kinds of field measurements are necessary for evaluating groundwater impact in a numerical groundwater in a permit application process for mining operations.

1.2 Limitations

The project is limited to using data from field measurements from two permit application processes for expansions of Kankberg mine conducted by companies Mark & Miljö Hydrosense AB and Bergab. These field measurements, includes pumping tests and monitoring of groundwater levels in soil and bedrock. The open data used in the first version of the numerical model is limited to maps from the Geological Survey of Sweden (SGU), The Land Survey (Lantmäteriet), Swedish Agency for Marine and Water Management (Havs- och vattenmyndigheten) and data from the Swedish Meteorological and Hydrological Institute (SMHI). No additional field work will be made from the project and no ecological impacts regarding the drawdown from mining operations will be considered.

The numerical model will constitute a MODFLOW finite difference numerical groundwater model implemented in Python. General limitations include the characteristics of making a case study, examining only the expansion between depths 600 to 1000m for the Kankberg site. The groundwater model will be based on a continuum model and individual fractures will be taken into consideration accordingly. Ecological impacts regarding water from mining activity will not be considered and the draining

of soil layer will also not be considered in the project.

Ethically, the study is not posing any risk of bias, since the authors have no beforehand connection to the company Boliden AB, and no economical compensation are involved. Certain information is withheld from the authors throughout the project to avoid bias when creating the early versions of the numerical model.

2

Theory

2.1 Hydrogeology in bedrock

Crystalline bedrock has properties like low primary porosity and permeability but can still act as local aquifers due to its secondary porosity (Ofterdinger et al., 2019). The secondary porosity consists out of faults, fractures and joints which are the attributes that can be described as the water-bearing discontinuities. The faults, fractures and joints have is a result of historical natural events that has caused structural deformations in the bedrock. In addition to these events, weathering can also increase the possibility of groundwater flow in present fractures. When looking at the hydraulic possibilities of the primary and secondary porosity, it can be assumed that it generally varies with depth. A study i Sweden showed that several kinds of bedrock had decreased hydraulic conductivity with depth (Statens rad for karnavfallsfragor (KASAM), 2005).

Infiltration from the soil to the bedrock occurs mainly where fractures are hydraulically connected to a permeable soil aquifer or in locations with heterogeneous soil (Olofsson, 1994). The contact zone of the soil and bedrock is of great importance in order for infiltration to occur as well as the presence of local fractures. Depressions by local fractures, can accumulate sorted and conductive material that results in more infiltration. In some cases, a layer of silt can sit on top of the bedrock that will block the infiltration due to the smaller hydraulic conductivity of the material. When modelling groundwater flow in bedrock aquifers, the recharge to the bedrock may be given as a boundary condition or it may be included in the modelling by using hydraulic properties of the soil and bedrock (Rodhe and Bockgård, 2006).

The groundwater flow in a crystalline bedrock is restricted to the fractures and can be assumed to be laminar (Gustafson, 2012). The flow is dependent on the fracture geometry and network of other fractures. The fractures are not planar but have structural surfaces with contact points which transfer the stresses within the rock material (Gustafson, 2012). It is within the opening of the rock, the aperture, that the flow occurs and therefore the aperture is one of the governing factors of the flow, which differs from soil where the water flows in the voids between the soil particles. Depending on the case and scale of the area of interest, either viewing the bedrock as a homogeneous continuum or as a network of planar structures can be more useful. In this case, viewing it as a homogeneous continuum can be considered similar to how soil material can be viewed. Since the geometry of the fracture is

correlated to the flow within the fracture, it can be assumed that larger fractures conduct more water than smaller fractures. Although, treating fractured bedrock as a homogeneous continuum is always a simplification of reality.

Estimation of the inflow into an underground construction is difficult as the rock fractures are unevenly distributed and therefore creates a inflow that is unpredictable (Gustafson, 2012). Simplifications must be made to enable predictions, and the certainty of calculated inflow rates is low. Calculating the inflow to an underground construction, such as a tunnel or a mine, could be made by simplifying the construction to a well. The well should have a radius of half of the diagonal in the rock cavern plane.

2.2 Groundwater modelling

There are several ways of conducting a groundwater model and they differ in methodology and outcome (Fetter, 2014). Analog scale models where important tools before digital computers were widely available. They can be used to visually simulate aquifer properties by constructing a physical model with porous media by e.g. (Fetter, 2014), adding dyed water to visualize the flow through the media. This type of models was particularly important in the 1960s (Anderson et al., 2015). The disadvantages with scale models are the lack of flexibility to change material or aquifer properties, there is also a need for storage of the model and material costs. Mathematical, or analytical, models on the other hand, are based on finding a solution of basic ground-water equations. Darcy's law is a mathematical and analytical model typically used for modelling groundwater flow. The model needs boundary conditions and an initial state in order to solve the problem. Simplifications are necessary for solving Darcy's, like set hydraulic parameters. When a higher level of detail is wanted in the model parameters, a more complex model is needed. A numerical model is therefore necessary when modelling groundwater sites with complex boundary conditions or where variation in parameters wants to be captured.

A numerical model solves a groundwater flow equation as stated in Equation 2.4. The equation represents three-dimensional groundwater flow in transient state for homogeneous and anisotropic conditions (Anderson et al., 2015). It is based on the water balance equation (Equation 2.3) and Darcy's law (Equations 2.1 and 2.2) that relates specific discharge to a head and a hydraulic conductivity.

Darcy's law:

$$q = -K * \mathbf{grad}h \tag{2.1}$$

q=specific discharge
K=hydraulic conductivity tensor
grad *h=gradient of head*

Darcy's law rewritten:

$$q = -K_{x,y,z}\frac{\partial h}{\partial x, y, z} \tag{2.2}$$

q = specific discharge
$K_{x,y,z}$ = hydraulic conductivity tensor
$\frac{\partial h}{\partial x,y,z}$ = hydraulic gradient in x,y,z directions

Water balance equation:

$$\frac{\partial q_x}{\partial x} + \frac{\partial q_y}{\partial y} + \frac{\partial q_z}{\partial z} - W^* = -S_S\frac{\partial h}{\partial t} \tag{2.3}$$

$\frac{\partial q_x,y,x}{\partial x,y,z}$ = *flux in x,y,z direction*
W^* = *sink or source*
$S_S\frac{\partial h}{\partial t}$ = *specific storage dependent on change in head over change in time*

Resulting in numerical flow equation:

$$\frac{\partial}{\partial x}(K_x\frac{\partial}{\partial x}) + \frac{\partial}{\partial y}(K_y\frac{\partial}{\partial y}) + \frac{\partial}{\partial z}(K_z\frac{\partial}{\partial z}) = S_S\frac{\partial h}{\partial t} - W \tag{2.4}$$

W = volumetric inflow rate from sources and sinks
K = hydraulic conductivity in x,y,z direction respectively
h = head
Ss= specific storage in aquifer

2.2.1 Workflow of groundwater modelling

The workflow of doing a groundwater model can be generalized and applies to most kinds of modelling (Anderson et al., 2015; Fetter, 2014). The main idea is to define the purpose of the model and collect the necessary data available to be able create a conceptual model, and then select a modelling design. After the construction of the initial model, an iterative process begins with calibrating and validating the model to the available data. A sensitivity analysis should be conducted to gain knowledge of the uncertainties of the model. As a last step, results can be extracted an evaluated. The workflow is illustrated in Figure 2.1.

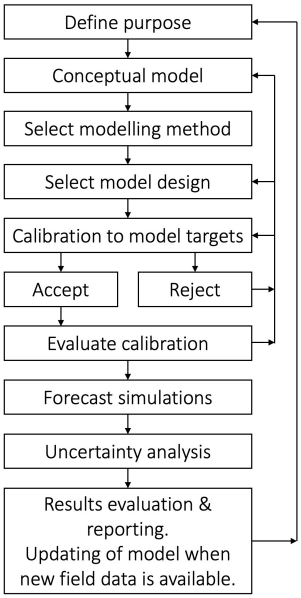

Figure 2.1: Workflow of groundwater modelling. Inspired by Anderson et al. (2015).

2.2.2 Conceptual model

To be able to make a numerical model of a groundwater system a lot of data and knowledge of the site and processes are needed. The data collection and processing are usually what is described as developing a conceptual model (Anderson et al., 2015). A conceptual model should include information about the site regarding the stratigraphy, the water system and anthropogenic aspects of the site to different extent. A more detailed and accurate conceptual model could have a higher probability of producing more reasonable results in a numerical model, although Fetter (2014) means that a conceptual model could never cover every detail within the system.

Important components regarding the soil and rock system and water system should be included in a conceptual model (Anderson et al., 2015). This includes data and knowledge about geologic properties, vegetation, hydrogeology including groundwater flow, sinks and sources as well as climate aspects such as precipitation. The result of conducting a conceptual model is usually presented in illustrations, diagrams, and tables to effectively communicate the site conditions.

2.2.3 Boundary conditions in model design

Boundaries in terms of groundwater modelling include the different hydraulic features of the site (Anderson et al., 2015). This could be for example the groundwater table, bodies of surface water, impermeable areas or divides in the groundwater flow. Hydraulic boundaries considered are both the ones along the perimeter of the

problem domain, and the internal boundaries.

In general, boundaries can be described as specified head, specified flow, and head-dependency boundaries, also known as Dirichlet, Neumann and Cauchy conditions respectively (Anderson et al., 2015). The Dirichlet conditions, i.e. the specified head boundary, are the boundaries in a model where the heads are known and set to a specific value. Since heads can vary, different specified heads can be set throughout the model. Although, when a head is the same along the entire boundary, it's usually called constant head boundary. The Neumann conditions are the specified flow boundaries, where the derivative of head over time is set. An example is the special case of no flow boundary where the flow is equal to zero. The flow in this case is calculated from Darcy's law. The Cauchy conditions is a boundary which is head dependent. The flow is calculated with Darcy's law using the gradient between a specified head outside the boundary and the head that the model has computed at the boundary.

The upper boundary is usually defined as the water table. Depending in what conditions model should evaluate, the upper boundary could be set to the most relevant one out of Dirichlet or Neumann conditions. For steady-state modelling, the Dirichlet condition should be used since there should be no change of head over time. But if a change in recharge is modelled, i.e. the specific flux, then a Neumann condition is the most accurate.

2.2.4 Calibration

Calibration of a groundwater model consists of varying the parameters until results become similar to known data (Fetter, 2014). Oftentimes the models are calibrated to steady state groundwater heads, initially by comparing the model outputs to a water-table or a potentiometric-surface map. Anderson et al. (2015) describes the calibration process in the terms of history matching, meaning that parameters are adjusted until they are both reasonable and produces results that match field observations sufficiently. The model quality is highly dependent on the quality of the input parameters, which is why the calibration step is of great importance to apply the quality of the parameters to the model (Hölting and Coldewey, 2019). One of the most common modelling errors are assumed to be that not enough time is spent on calibration (Anderson et al., 2015).

A way to calibrate is to use the root mean squared error (RMSE) which is common to use for steady-state models and for transient models (Equation 2.5). A way of using RMSE is to set a criterion in percent, based on the fault tolerance and to plot the simulated values on one axis and the measured ones on the other. The location of the plotted coordinates is compared to a 1:1 line to find systematic errors such as overestimating and underestimating the result.

$$RMSE = \frac{1}{n}\left[\sum_{i=1}^{n}(h_m - h_s)_i^2)\right]^{0.5} \tag{2.5}$$

2.2.5 Uncertainties and model sensitivity

Uncertainties in groundwater modelling relates to both uncertainties of the model, but also in the prediction of the future conditions (Anderson et al., 2015). Differences to the simplified conceptual model and observational errors for the calibration are model uncertainties that needs to be addressed. The extremes are either an oversimplified model or a overly complex model where the aim should be somewhere in between by setting a minimum total error between the extremes. Otherwise, the issues of uncertainty for an over simplified model will be due to errors in the parameter settings and for an overly complex model from overfitting. The uncertainties regarding the future conditions of stresses and properties which can either be "known unknowns" or those things which cannot be anticipated "unknown unknowns".

A sensitivity analysis is oftentimes conducted along the calibration of the model, to gain knowledge of how changes in model parameters impacts the results (Fetter, 2014). The model parameters that are changed during the sensitivity analysis are generally the hydraulic parameters and the boundary conditions. Typically, one of the calibration parameters are changed at the time whilst the others are fixed when conducting a manual analysis (Anderson et al., 2015). The calibrated parameters are usually changed in sequences of increasing or decreasing the value by some set percent. The reason to conduct a sensitivity analysis is to determine which parameter that affects the result the most, thus revealing the weaknesses and uncertainties of the model.

2.2.6 MODFLOW

Simulating groundwater flow can be conducted by solving with equations in a finite numerical model like MODFLOW (Harbaugh, 2005). The model uses a block-centered finite difference method to solve flow problems. Previous finite-difference models were used by the U.S. Geological Survey (USGS) by Trescott, Pinder, and Larson from 1976. The development of MODFLOW was done as a consolidation of previous models to create a simpler and more modifiable code. MODFLOW has been developed in several versions since 1983. The packages used as subroutines are programmed in Fortran and are the base of the modular structure of the code.

MODFLOW-2005 can be used for both two- and three-dimensional cases and the different aspects of groundwater flow modelling are divided into packages (Harbaugh, 2005). These packages simulate aspects like internal flow processes, the impact of stress such as recharge, rivers, wells and drains, but also packages that works as solvers for the problem specification.

There are different ways of utilizing MODFLOW. For example, can the method can be used in Python with the Flopy package (Bakker et al., 2016) where groundwater flow problems are solved with single lines of codes. Another option is to use software with graphical interface like ModelMuse (Winston, 2019) and Simulating MODFLOW (Chiang and Kinzelbach, 1991). In Python, a script is created to solve numerical problems and additional libraries can be used together with Flopy to work

with geo-spatial information (GIS), performing data analysis and creating graphics Bakker et al. (2016). The benefit of using graphical interface software is mainly the interactive environment that does not require any programming as Flopy do (Winston, 2019).

In Flopy, several steps are taken to run a model (Bakker et al., 2016). Packages are used to make a discretization of the problem area, as well as setting up initial conditions and boundaries. Geo-spatial information can also be used by utilizing available Python packages. Several other packages can be used to simulate pumping wells, discharge and recharge. There are also options to solve steady-state and transient state models over time. After these steps, solvers are imported to solve the model. Additional packages can also be added to visualise the results with graphs.

2.3 Regulations of groundwater and mining

The Swedish environment is protected by law and activities that can negatively impact the environment are regulated by the Swedish Environmental Code (Michanek and Zetterberg, 2017). The Environmental Code came in to force in 1999 as a replacement and consolidation of the previous set of laws regarding the environment, nature and water. An activity that could affect natural water systems is referred to as a water operation in the Environmental Code. Water operations are categorised as one of the three concepts: construction in water; a raw water source used for drinking water production; or dewatering of land. The consequences of water operations are physical effects of the surface or groundwater environment by an increase or decrease of the amount of water on a site, or a change of the natural path of the water on site.

Mining activity is unavoidably associated with impact on land and nature (Jain et al., 2016). The removal of inflowing water into the mine is a typical example of a water operation. The removal of the water that leaks into the mine results in a dewatering of the surrounding ground (SOU, 2022), which can affect wildlife and ecosystems dependent on certain groundwater levels for accessing water (Jain et al., 2016). The consequences could be dry wells in the surroundings, affecting e.g. private wells used for drinking water. Mining activity could also result in the need of redirection of water courses due to the location of the ore findings, which can have an effect on the landscape (SOU, 2022) and dry out wetlands. Mining operations require water for cooling, cleaning and in processing of the ore, and the groundwater that is removed when dewatering the mine could thereby be used for these purposes (Wessman et al., 2014). Oftentimes lower quality water is accepted in the processing, making it possible reuse the water in several operations.

2.3.1 Permit process

Activity that potentially could pollute groundwater or lower the groundwater table requires a permit from the Land and Environmental Court in Sweden (Lewis et al., 2013). The process starts with requesting a permit at the county board and involving all stakeholders that could be affected, including municipalities, governmental agencies and the public. The relevant actors and affected stakeholders should be able to express their opinion, either through writing or at a public hearing.

The permit is approved by the Land and Environment Court based on the presented evidence from the applicant actor of the water operation (Michanek and Zetterberg, 2017). There is no specified form for the permit application, which means that the actor has to know what type of evidence to prepare and bring to the court. However, some things are mandatory, such as an environmental impact assessment (EIA). The EIA has the purpose of describing the environmental impact that the planned operations will result in, including health and environmental effects on humans, nature, water, landscape and cultural environments, water and land conservation and general conservation of resources and energy. The EIA should also include transparent communication to relevant stakeholders, inviting to possible involvement in the process. Besides the EIA, the permit application must include foreseen risks, possible impacts on nature and environmental water, and suggested solutions and prevention of the risks and consequences (Lewis et al., 2013). The obligation to provide evidence is strict, which results in the need for thorough investigations before any water operations start.

The demands for the court to approve a permit for water operations are involving several parts of the Environmental Code beside the demand low impact of the water on the site (Michanek and Zetterberg, 2017). The general rules of consideration in chapter 2 sets out regulations for location and precaution or prohibition of the water operation. The water operation should also be in line with the domestic regulations in chapter 3 and 4 and the rules about nature protection in chapter 7. Approving the water operation also includes considering the societal economic feasibility of the operation along with the effect on other water operations present and the fishery on the site. The consideration is requiring an economic calculation of the damages and effect on the site compared to the economic value creation of the water operation. According to Michanek and Zetterberg (2017) economic value in untouched nature should be able to be calculated with respect to economic resources intended for protection of the landscape, species or ecosystems or in terms of expected tourism at the site.

The permit is approved with addition of requirements for the water operation, which could be e.g., the total quantity of groundwater per time unit from aquifer dewatering (Michanek and Zetterberg, 2017). If the actor fails to follow the requirements in the legal permit or proceeds with a water operation before having gained legal force, the permit is withdrawn and consequences are determined. The consequences can be sanctions such as fines but also prison sentence in severe cases according to 29 c. 4§ in the Swedish Environmental Code SFS 1998:808.

3

Case study description

The Kankberg mine is Västerbotten county, northern Sweden in the municipality of Skellefteå Voigt and Bradley (2020). The area is historically associated with the company Boliden Mineral AB, since the first open pit mine located in Boliden, that was in operation from the 1930's to 1967. The Boliden area is also home to two other underground mines, the Renström mine and Kristineberg mine. The Kankberg mine currently consists out of four main parts, one open pit, two underground mines and an access ramp.

The Kankberg mine is an operating underground mine since 2012 (UM2012) between depths -320m and -530m. It is situated in Eastern Åkulla, southeast to the open pit, accessed by a ramp from the bottom of the old structures of the Kankberg mine. The old Kankberg mine started operations in 1966-1969 as an open pit mine (OPM1966), see Figure 3.1. An expansion was made in 1988 to continue the mine as an underground mine (UM1988) which operated between until 1998 down to approximately depth -320m.

A process has started to get a permit to start mining below and above UM2012 since the findings are predicted to be feasible (Voigt and Bradley, 2020). The permit of the expansion includes expansion in the depths -50m to -300m and between depths -600m to -1000m. For this project, the expansion between -600m to -1000m will be investigated (UM20XX). From here on, the mines will be referred to as in table 3.1.

Table 3.1: Abbreviations of the mines in the project.

Name	**Depth from ref.point**	**Explanation**
OPM1966	from surface to -50m	Open-pit mine (1966-1969)
UM1988	from -50 to -320m	Expansion of open-pit mine (1988-1997)
UM2012	from -320 to -530m	Kanberg mine, underground mine from 2012
UM20XX	from -600 to -1000m	Investigated expansion of UM2012

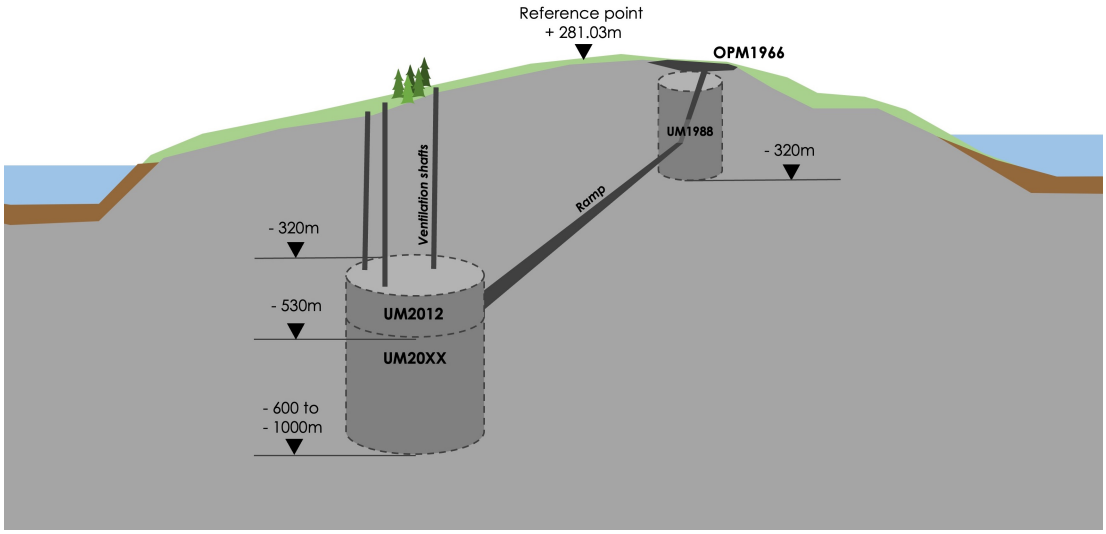

Figure 3.1: Visualization of the mines in Kankberg.

3.1 Open-source data (DSOPEN)

The open-source data set included several products and files from Swedish authorities and agency's as listed in Appendix A.1 and A.2. The data set also included values on precipitation and evapotranspiration from SMHI (2024) and expert knowledge on parameters such as hydraulic conductivity.

3.1.1 Bedrock geology

The Kankberg area is located in the District of Skellefteå is located between the nothern Västerbotten and southern Norrbotten, which is a part of the Fennoscandian Shield (Kathol and Weihed, 2005). The major geological unit in the District of Skellefteå is the Palaeoproterozoic rocks such as the Palaeoproterozoic Svecokarelian unit. The Svecokarelian units comprises of intrusive rocks and supracrustal rocks whereas the supracrustal rocks are divided into the Bothnian Supergroup and Skellefte, Arvidsjaur and Vargfors groups. Bothnian Supergroup consists out of mainly gneissic or migmatized metagrey wackes, whereas the Skellefte group includes subaquaeous volcanic environments.

The bedrock specifically around the area of Boliden and Kankberg are built of folds of the Skellefte and Bothnian groups (Kathol and Weihed, 2005). These groups have an anticline with a striking axle in north-east-south-west direction. The mined ore is located in the host rock consisting of feldspar porphyritic subvolcanic dacite at the Skellefte group stratigraphical top. In the area, the Bothnian Supergroup is also present, consisting of volcanic sandstones and sedimentary rocks. The area consists of both ductile and brittle deformation zones. Within the surroundings of Kankberg mine, several types of bedrock units can be identified such as porhyric dacite-ryholite, wacke and hydrothermally altered granite as can be seen in figure 3.2.

In an investigation from 1993, fractures were found in the area generally in the striking directions north-west to south-east and other sets of fractures are in north-east to south-west direction a north-north-west to south-south-east (Wladis, 2009). Expert help have estimated the hydraulic conductivity in the bedrock in the district as presented in Table 3.2

Table 3.2: Hydraulic conductivities, hk, of Swedish glacial till and crystalline bedrock according to expert help.

Layer	**hk (m/s)**
Glacial till	10E-5 - 10E-7
Bedrock -50m	5*10E-7
Bedrock -100m	5*10E-8
Bedrock -200m	1*10E-9

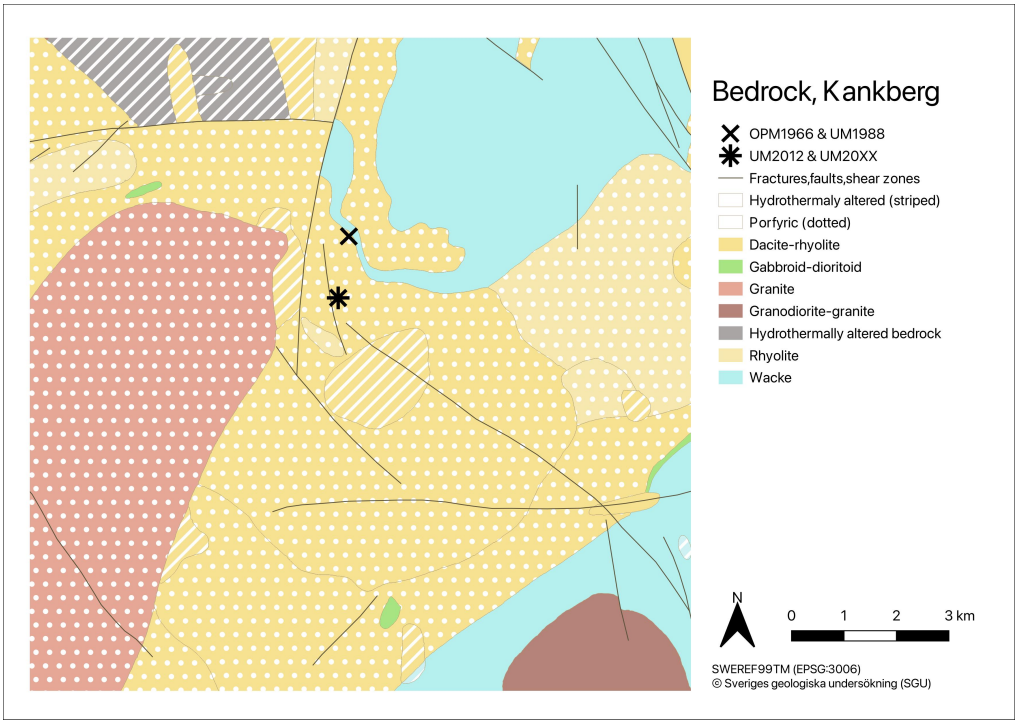

Figure 3.2: Bedrock in Kankberg, Skellefteå.
Map used: *Berggrund 1: 50 000 - 1:250 000 ©SGU*

3.1.2 Quaternary deposits

The geology in the area mainly consists out of glacial till with some local areas of peat as can be seen in figure 3.3. The thickness of the soil cover varies from surfacing bedrock up to around 22 m according to the ©SGU map Jorddjup 10x10m resolution.

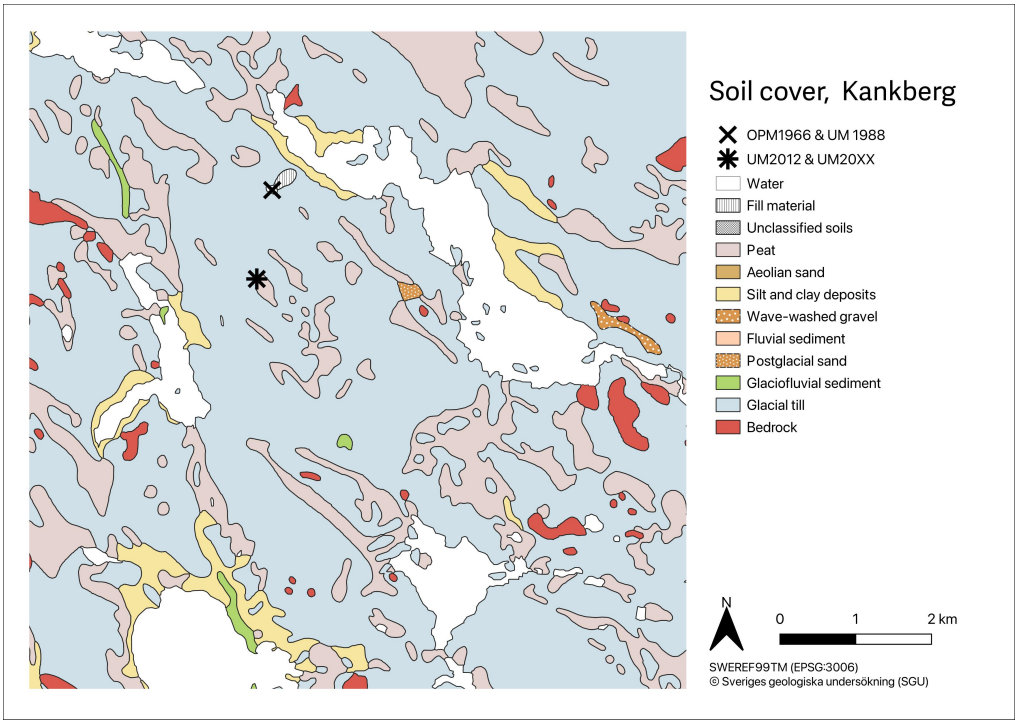

Figure 3.3: Soil types in Kankberg, Skellefteå.
Map used: *Jordarter 1: 25 000 - 1:100 000 ©SGU*

3.1.3 Topography and hydrology

The topography in the area around Kankberg is visualized in the contour map in Figure 3.4 which is based on the topography raster from SGU. The OPM1966 is located at around 270 m in RH2000. The slopes in the western part of Kankberg and in the northeastern part are steeper than the more southern part of the hill.

3.1.4 Hydrogeology

Groundwater levels have been measured by SGU at a number of wells in the area (Figure 3.4). The reported measurements indicate groundwater levels in the area to approximately 2 - 23 meters below ground level. The wells are located near the lakes and on a hillside. Bodies of surface water in the area are Stavträsket and Bastuträsket with the respective water levels of 191m and 209m above sea level according to The Land Survey via Eniro (2024). Several smaller lakes in the area of interest are Klocktråsket, Bastutjärnet, Gillervattnet, Avatjärnet, and Innersttjärnet as well as the old open pit mine Western Åkulla that water filled. Streams are present in the area, some of which runs through local mires.

3.1.5 Hydrology

The investigated area consists out of four smaller catchment areas that are identified by SMHI and Swedish Agency for Marine and Water Management (SMHI and Havs- och vattenmyndigheten, 2024) and are presented in Figure 3.5. These four catchment areas discharge water into lakes and streams nearby, illustrated in Figure 3.5. The catchment 28912 discharges into the outflow of Stavträsket, 28989 to the inlet of Bastuträsket, 28970 to the outflow of Bastuträsket and 28785 to the outflow of Gillervattnet. The OPM1966 and the UM1988 are located in the 28970-catchment area and the UM2012 with the expansion UM20XX are located in catchment 28912. The average annual precipitation is similar between the areas. Between years 2010-2022, the annual precipitation and estimated evapotranspiration has been evaluated, presented in Table 3.3.

In the investigated area, several mires have been identified by The Land Survey via Eniro (2024). These overlap well with the larger consistent peat areas found in figure 3.3. A mire is a kind of wetland where dead vegetation is not fully degraded but rather are converted to peat (Rova and Paulsson, 2015). New vegetation is growing on top of the mire and therefore continues the cycle of producing peat. For mires to form, water needs to be present. For instance, a mire can be found as an overgrown lake or in areas that regularly are flooded or in areas where groundwater are seeping out as surface water.

Recharge is impacted by factors such as slope and soil cover. Since Kankberg is a hill, slopes surround the mines in the area. The top of the hill is flatter and towards the larger lakes steeper slopes are found (Figure 3.4. Larger slopes result in less recharge due to runoff, causing insufficient time for infiltration (Yeh et al., 2009). Recharge at the foot of a hill can either be where most recharge occur, but it can also vary depending on direction (Grinevskii, 2014). In flat surfaces and the top part of a slope results in some recharge, but generally less than in the slopes.

Table 3.3: The average yearly precipitation and evapotranspiration in the catchment areas 28912 and 28970 between the years 2012-2022 (SMHI and Havs- och vattenmyndigheten, 2024).

Parameter	**28912 (mm/year)**	**28970 (mm/year)**
Precipitation	723	730
Evapotranspiration	448	404

3.2 Site specific data from field measurements

Field measurements have been collected in the area with the purpose of retrieving mining permits for the mines UM2012 and UM20XX as presented in 3.6. The first number of measurements were collected and reported in the year of 2008 and the second round in 2022. The reference point has been set to +281,03m in RH2000.

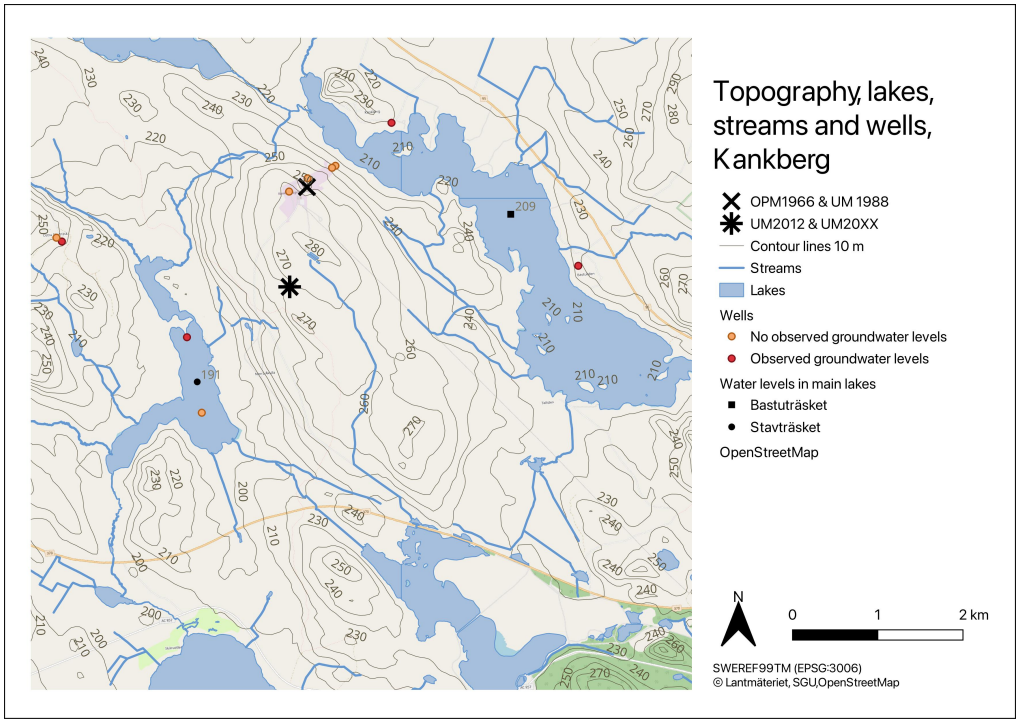

Figure 3.4: Contour map of Kankberg, Skelleftea.
Maps used: *Grid2+ and GDS-Fastighetskartan vektor ©The Land Survey, Brunnar latest ©SGU, and OpenStreetMap©*

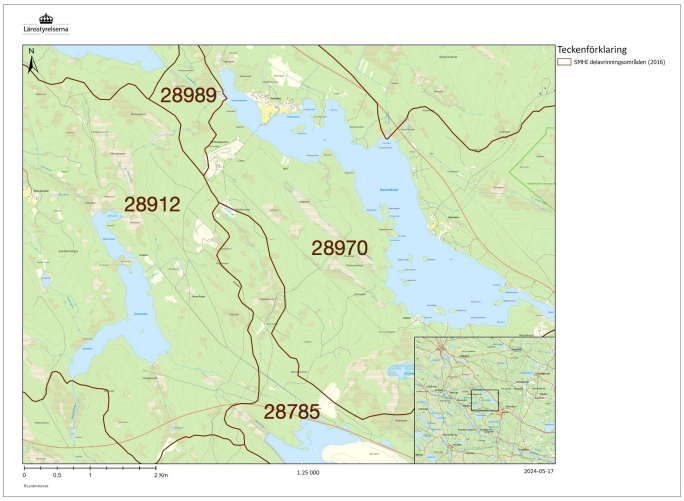

Figure 3.5: Catchment areas in Kankberg.
Map used: *Vattenkartan ©The Land Survey and County Administrative Board (Vatteninformationssystem Sverige (VISS), 2024)*
Note: SUBID added for each catchment area, brown lines represent the catchment area boundaries.

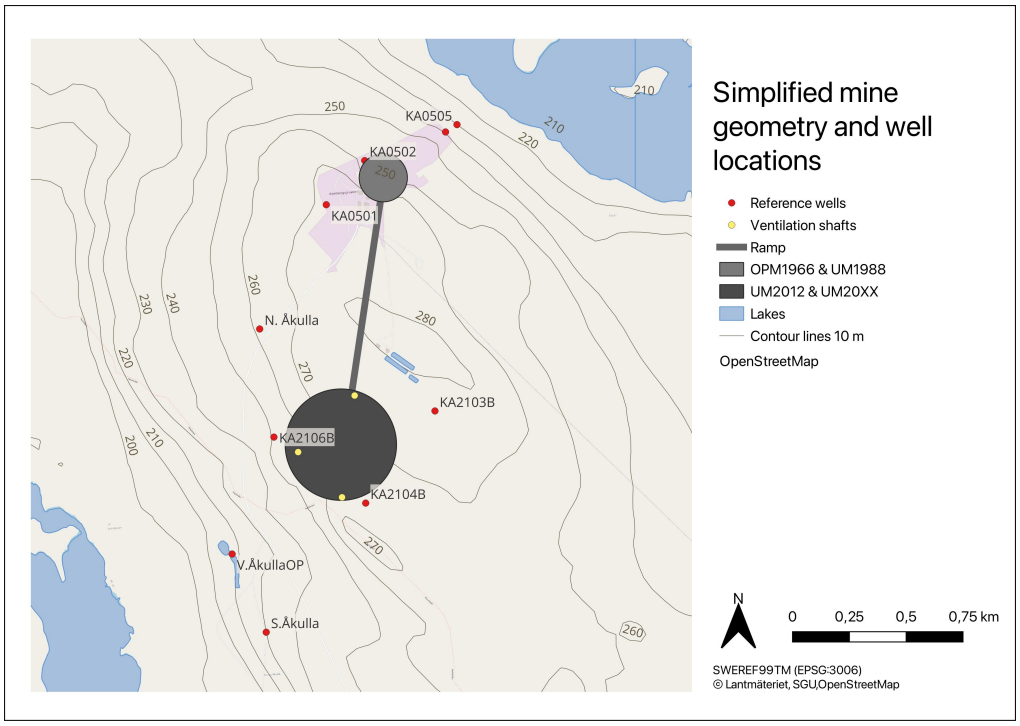

Figure 3.6: Simplified mine geometry and wells from field measurements. Maps used: *Grid2+ and GDS-Fastighetskartan vektor ©The Land Survey, Brunnar latest ©SGU, and OpenStreetMap©*

3.2.1 Data set 2009 (DS2009)

The data set for the permit application for UM2012 was collected in 2009 and will be called DS2009 following. Five groundwater observation wells were drilled in close proximity to the open pit mine OPM1966 as seen in Figure 3.6. Three were drilled in the bedrock (KA0501, KA0502, KA0503) and two were in drilled into the soil layer (KA0504, KA0505) (Wladis, 2009). The first undisturbed measurements were collected in 2005 and the second round of measurements in 2008. Two additional wells were drilled before the start of an exploration drift in 2008 and are called Northern Åkulla and Southern Åkulla. The groundwater levels were measured undisturbed, and results can be found in figure 3.4.

In the exploration drift at -430m from reference level, several core drillings with different lengths were made to investigate the direction of the ore (Wladis, 2009). The drillings were not conducted to give the correct hydrogeological features in the bedrock and no directions were noted. Although, a bulk hydraulic conductivity was estimated based on pressure tests of the drillings. The evaluated bulk hydraulic conductivity was found to be low like a dense bedrock, and the result is presented in 3.5. In the same table, other results from different tests are presented.

Table 3.4: Measured groundwater levels around Kankberg in RH2000. *surface level at specified well(m), ** groundwater levels (m) measured 2005-12-15 and measured 2008-01-22 for KA0501-0505 and during an unspecified day in 2008 for N. Åkulla and S. Åkulla.

	0501	**0502**	**0503**	**0504**	**0505**	**N. Åkulla**	**S. Åkulla**
Well type	bedrock	bedrock	bedrock	soil	soil	bedrock	bedrock
sl*	272	255	236	236	228	260	235
gwl -05**	244,7	233,38	229,98	231,72	227,13	-	-
gwl -08**	236,2	213,44	255,18	228,32	224,96	250-255	225-230

Table 3.5: Evaluated hydraulic conductivity, k, in Kankberg area from several field measurements.

Location	**k (m/s)**	**Bedrock depth**	**Average k (m/s)**
Pumping test in well KA0503	5,20E-09	0 to -200m	3,48E-08
Pumping test wells N. Åkalla and S. Åkalla	2,00E-08	0 to -200m	
Analysis on wells in bedrock	5,60E-08	0 to -200m	
Calculated from inflo to OUM1966, UM1988	5,80E-08	0 to -320m	
Core drilling tests in exploration drift	6,10E-10	- 430 m	6,10E-10

3.2.2 Data set 2022 (DS2022)

Additional data was available for the permit process 2022 (Table 3.6. In addition to the seven wells KA0501-0505, Northern Åkulla and Southern Åkulla, additional wells have been drilled for groundwater measurements both in the soil and the bedrock as seen in Figure 3.6. Three of the additional wells have been hydraulically evaluated with pumping tests as well as the previous wells as presented in Table 3.8. All wells in figure 3.8 have depths ranging from 199-225m. Groundwater levels in KA0501-0505 have been almost stabilized and levels from 2008 found in table 3.4. Inflow into the structures of the mine have also been stabilized and measure as seen in Table 3.9.

The measurements in KA0503-0505 shows that the groundwater levels for soil have been stabilized as well as in bedrock for KA0503 (Appendix A.3). The KA0503 also shows groundwater levels in the bedrock that exceeds the ones in the soil for KA0504.

Table 3.7: Measured groundwater levels for the permit 2022 (RH2000). *surface level at specified well(m), ** groundwater levels (m) measured in September 2021.

	2103B	**2104B**	**2106B**	**N.Åkulla**	**S.Åkulla**	**V.Åkulla**
sl*	266	266	251	260	23	217
gwl**	211,1	203,3	179,9	207,2	221	201

Table 3.6: Content in data sets DS2009 and DS2022 used in the model method. "* T = transmissivity test that were disregarded in this project. ** pumping tests & recovery test, infiltration & recovery, pulstest. ***pumping tests & recovery test **** 20 flow & 7 pressure tests from exploration drift *****calc for both (-50)-(-320)m and (-600)-(-1000)m since the water in V.Åkulla will flow into an exploration drift at level 180 which will be a part of the -50 level, one of the calculations is just the OPM and the other OPM and the exploration drift"

Category	**DS2009**	**DS2022**
Groundwater levels	Ö. Åkulla old open pit mine (1 meas.) V. Åkulla old open pit mine (1 meas.) KA0501-0505 wells (2 meas. per well) Wells archive (1 meas. per well)	Ö. Åkulla old open pit (+1 meas.) V. Åkulla old open pit (+ several meas.) KA0501-0505 wells (+1 meas./well) Wells archive (no additional) KA2103B, KA2104B, KA2106B wells (+ 1 meas./well)
Hydraulic conductivity evaluation	N. Åkulla (T*) (1 meas. **) S. Åkulla (T*) (1 p.t & 1 rec***) Core drillings (20 + 7 meas.****) Pumping test in unspecified wells	N. Åkulla (no additional) S. Åkulla (no additional) Core drillings exploration drift (no additional) Pumping test in unspecified wells (no additional) Well KA2103B, KA2104B, KA2106B (+1 p.t & +1 rec***)
Measured inflow for calculation of hk	OPM1966 & UM1988 (1 meas.) Core drillings in exploration drift (20)	OPM1966&UM1988 (+1 meas.) Core drillings in exploration drift (no additional) UM2012 (+1 meas.) The three ventilation shafts (+1 meas./shaft) Ramp (+1 meas.)

Table 3.9: Measured inflow in Kankberg, 2021

Mine structures	**m^3/h**
Underground mine UM2012 and ventilation shafts	77,1
Ramp between -277 to -430m	2,5
Mines OPM1966, UM1988	15,7
Total	*95,3*

Table 3.8: Calculated hydraulic conductivities from all wells in Kankberg. * wells located in soil, all others are drilled into the bedrock. ** wells 199m long, evaluated by Wladis (2022)

Well	**Method**	**K (m/s)**
KA0501	Moench (1997) unconfined	8,20E-09
KA0501	Slugtest Bouwer-Rice	7,10E-07
KA0502	Slugtest Bouwer-Rice	6,90E-10
KA0503	Papadopulus-Cooper Confined (1967)	5,20E-09
KA0503	Moench (1997) unconfined	1,80E-08
KA0504*	Papadopulus-Cooper Confined (1967)	1,10E-06
KA0504*	Cooper-Jacob unconfined	1,50E-05
KA0505*	Papadopulus-Cooper Confined (1967)	6,30E-06
KA0505*	Cooper-Jacob unconfined	1,60E-05
KA2103B**	Drawdown	2,60E-08
KA2103B**	Recovery	2,80E-08
KA2103B**	*Average*	2,70E-08
KA2104B**	Drawdown	1,60E-08
KA2104B**	Recovery	1,70E-08
KA2104B**	*Average*	1,65E-08
KA2106B**	Drawdown	1,40E-07
KA2106B**	Recovery	1,10E-07
KA2106B**	*Average*	1,25E-07
Soil	*Average*	*9,60E-06*
Bedrock	*Average*	*9,81E-08*

3.3 Mine geometry

The geometry varies between the different structures of Kankberg mine and simplifications were needed for the conceptual model and modelling. The OPM1966 and UM1988 were assumed to be shaped as cylinders with diameters of 200m (and 100m for a sensitivity analysis) as presented in Figure 3.7 and 3.6. A circular shape was chosen as it best represents the impact of groundwater flow patterns. In reality, the

geometry if the mine is not in the shape of a cylinder in this area but rather in drifts from a ramp at different levels. From UM1988, a ramp with a decline connects to the central part of UM2012. The simplification for this was to make a horizontal connecting line from the bottom of UM1988 to the top of UM2012. The UM2012 has a complex geometry that was simplified to a cylindrical shape with a diameter of 480m. Since no geometry of the UM20XX was available, an assumption was made that the geometry would be similar to the UM2012 and that the diameter of 480m was used. The ventilation shafts were simplified to single cells in the grid that runs from the ground surface down to UM2012.

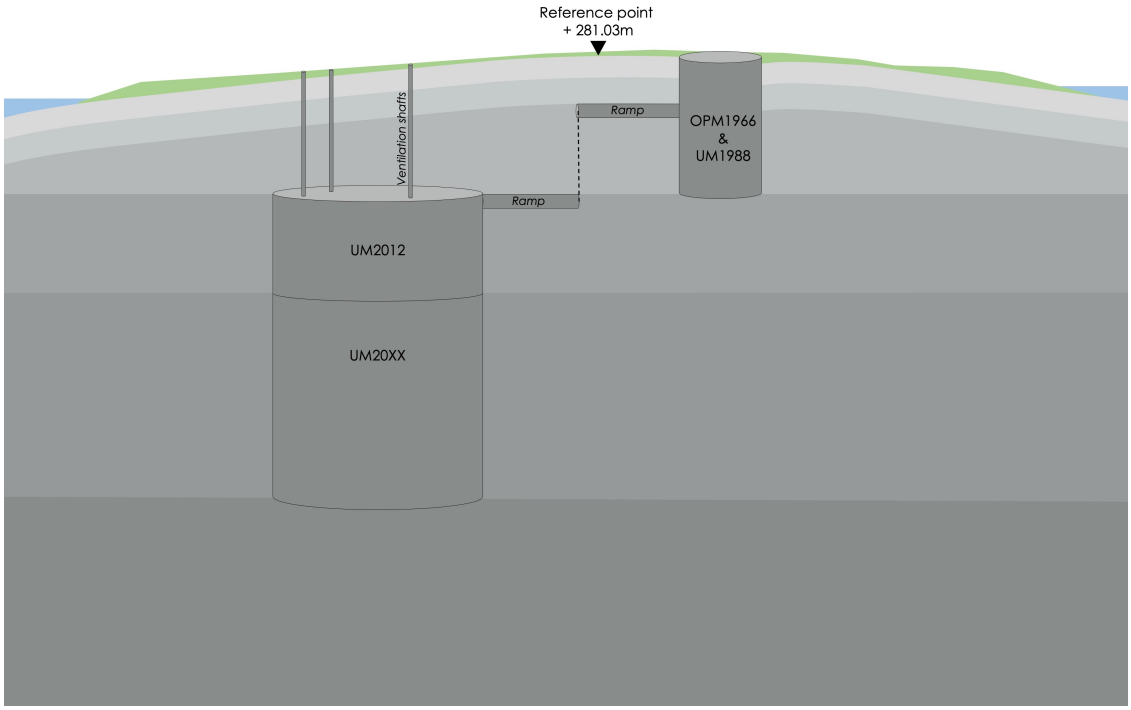

Figure 3.7: The geometries of the structures of the mine.

3.4 Conceptual model

The interpretation of the data collected and the relevant processes governing the groundwater flow in the area of the Kankberg mine can be seen in the visualized conceptual model in Figure 3.8. The processes included are the hydrological processes such as precipitation, evapotranspiration, runoff, recharge and the larger hydraulic boundaries which are the lakes. Groundwater flow and pressure distribution in the bedrock was interpreted as described by Gustafson (2012) for tunneling projects. The conceptualized underground structures of the mines are also presented in the figure, including the ventilation shaft, ramp and the areas where drifts of OPM1966, UM1988, UM2012 and UM20XX have been made or are planned. The conceptualization of the recharge and the layering of hydraulic conductivity is presented in Figure 3.9.

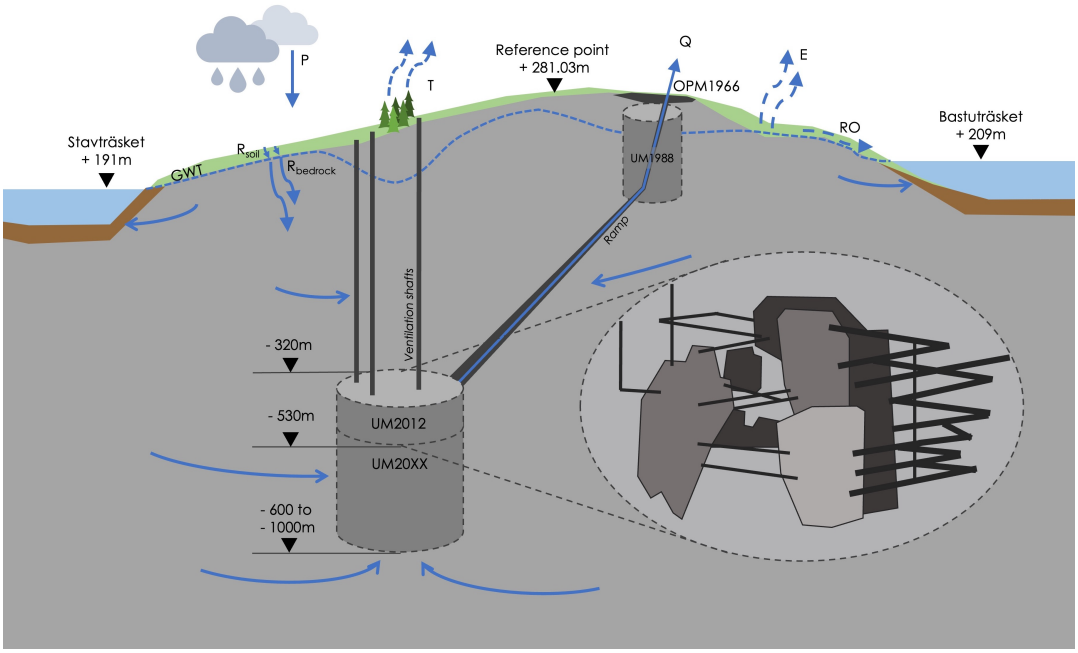

Figure 3.8: Conceptual site model. The UM2012 is modified from Voigt and Bradley (2020)

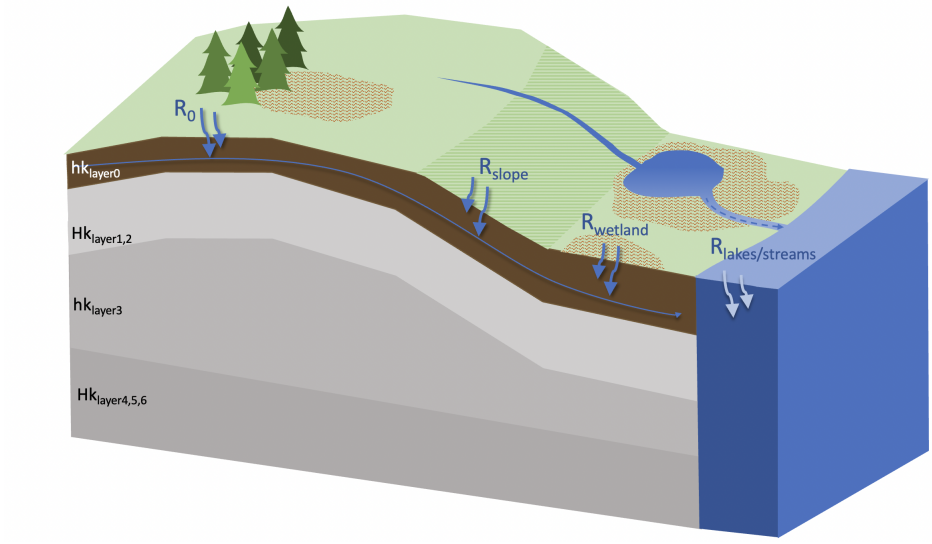

Figure 3.9: Conceptualization of parameters

4
Methods

The method for the project work included several steps. A literature research was made about groundwater flow in soil and bedrock, groundwater modelling and the legal and environmental aspects of impacting the groundwater during mining operations. Then, information and data were collected and a conceptual model was created. A general process of creating the numerical model was also made, to be able to systematically and without bias create numerous models calibrated with different data sets. Parallel to the modelling, geospatial processing was made to provide input for the models. Calibration and post processing was made prior to extracting the results. Finally, the results were compared in a qualitative evaluation regarding the economic value of the model accuracy. An overview of the methods used is presented in the flowchart in Figure 4.1.

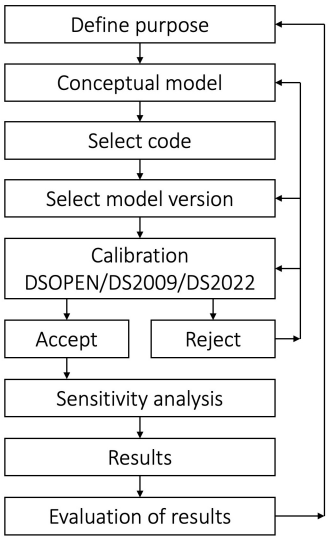

Figure 4.1: Overview of methods

4.1 Data collection for calibration

Geological and topographical data was used to build the model in Python. The open-source data files were retrieved from the the Swedish University of Agricultural Science (SLU, 2024) web-service "GET". GET contains shape- and tiff-files created by the authorities The Geological Survey of Sweden (SGU) and The Land

Survey. The data is based on investigations made by the authorities and is free of download for students and researchers. Data regarding the precipitation and evapotranspiration was downloaded from SMHI vattenwebben 2024. The files used for this project can be seen in Appendix A.1 & A.2.

Data for calibration of the numerical models were categorized in three datasets: Open-source data (DSOPEN), data from the environmental permit in 2009 (DS2009) (Wladis, 2009) and data from the environmental permit in 2022 (DS2022) (Wladis, 2022). DSOPEN includes all site-specific data that is available through authorities, concepts and processes within hydrogeology and other expert knowledge gained with experience of working with groundwater models. DS2009 refers to data from pump tests, core drillings, groundwater level observations and observed inflow into the operating parts of the mine. These measurements and observations were made for the environmental permit regarding the underground mine that went into operation 2012 (UM2012). DS2022 are referring to data from pump tests and groundwater level observations made for the environmental permit regarding the expansion of the mine that is not in operation yet (UM20XX).

4.2 Geospatial processing in QGIS

The data retrieved and used within the project was the elevation, soil depth, soil types and types of bedrock, listed in detail in Appendix A.1 and A.2. The highest resolution was chosen for all of the downloadable data.

All of the used rasters and shapefiles were processed in a GIS software. The files were clipped into the project domain area and were set to a 10 by 10 resolution, resulting in 600x698 rasters. The topography and the bedrock surface were interpolated with a Gaussian filter to support the model convergence. The contour map was made from the elevation grid with 10m space between the contours.

Several rasters were produced for the model. To retrieve the bedrock surface levels, the raster calculator was used in QGIS subtracting the soil depth from the elevation. A lake raster from the mv_riks file was made for setting boundary conditions. The rivers and streams were also compiled into one raster from the ml_riks file. To control recharge areas two rasters were produced, one with the peat covered areas as can be seen in Figure 3.3, and the other with the slope in degrees in the area calculated from the topography. The simplified geometry of the mines, ventilation shafts and the ramp was also made as vector layers in QGIS and was then converted into rasters for better control in the modelling.

4.3 Numerical groundwater modelling in Flopy

The aim of the numerical groundwater modelling was to predict impact on surrounding groundwater levels with the expansion UM20XX. The predictions were made using the three calibration data sets DSOPEN, DS2009 and DS2022 in a groundwater model.

The model approach was to develop three models, based on data listed in 4.1 from the three datasets, introducing UM2012 and UM20XX in steps. The approach is conceptually illustrated in 4.2. The process started with creating a functional groundwater model with site-specific open data (Model 1.0). The first calibration with DSOPEN resulted in a prediction of the impact of the UM1988, the connecting ramp, the ventilation shafts and the UM2012 (Model 1.1). The UM20XX were then added to predict the impact on groundwater levels connected to the expansion (Model 1.2). Two other models were then created with the base of Model 1, calibrating with DS2009 (Model 2) and DS2022 (Model 3), retrieving results for evaluation and comparison. The calibration data were not viewed by the authors before needed in the process, to build unbiased models. The most interesting result are retrieved when comparing Model 1.2, Model 2.2 and Model 3.2, all simulating the impact on groundwater levels with the expansion UM20XX, but calibrated with different data sets.

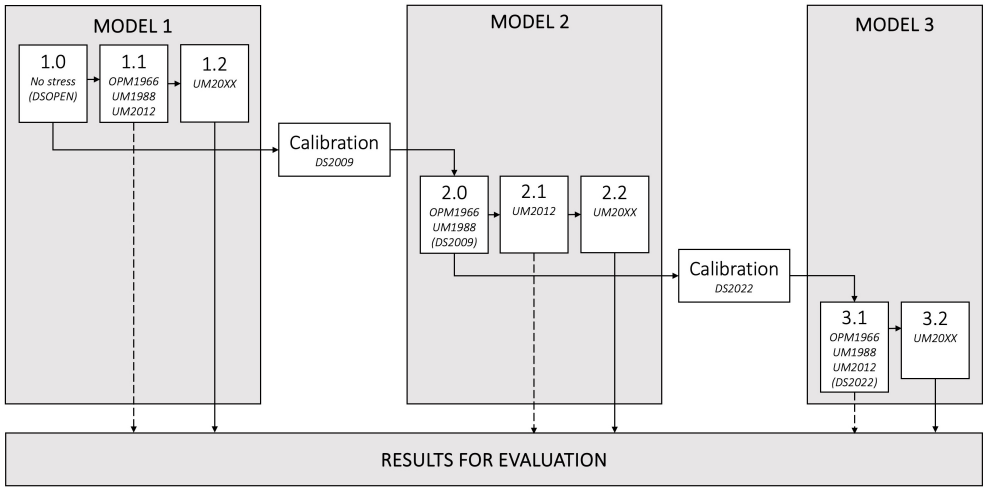

Figure 4.2: Model approach for numerical model development based on the stressors and datasets.

4.3.1 Geospatial processing in Python

The model components were mainly based on rasters, managed by the library Rasterio. Some of the rasters were processed in the Notebook, specifically to manage irregularities among the rasters and no-data cells. For example, the topography raster was processed by replacing the correct cells with an average water level of each lake.

Table 4.1: Data used for the different models in Figure 4.2 for Model 1 (M1), Model 2 (M2) and Model 3 (M3). *used as guidance in calibration, **used as guidance in calibration where no measured values were available.

Datasource	Data type	M1	M2	M3
DSOPEN	Raster files	x	x	x
	Well archive for strt	x	x	x
	Expert knowledge on hk	x*	x**	x**
DS2009	All available groundwater measurements		x	x
	Average hk		x*	
	Inflow UM1988		x	
DS2022	All available groundwater measurements			x
	Average hk			x*
	Inflow UM1988			x
	Inflow ramp			x
	Inflow UM2012			x

The bedrock raster contained no-data cells, generally in areas with lakes. Where the no-data cells intersect with the lakes, the soil depth does not affect the model due to the chosen boundary settings. Therefore, it was decided to replace the no-data cells with the topography to have a continuous bedrock raster. Although, a threshold value for the soil depth was set to stabilize the model. In this case, three meters was chosen as the minimal soil depth and in areas where that condition was not met, the bedrock surface was lowered. The reason why the bedrock was chosen to be changed instead of the topography was because the topography had a higher resolution and higher quality than the bedrock raster.

The visualisation of the rasters was made with the matplotlib library. In rasters containing model components such as lakes, rivers and wells, specific values were assigned for identification for each element, making it possible to change the settings for single elements.

4.3.2 Model setup and solver setup

The package Modflow was used to set up the model. Input parameters for the Modflow package was a model name, the filepath to the executable file, a name for the model workspace as well as the version of modflow to be used. The used version was the 'mfnwt' indicating that the MODFLOW-NWT solver was chosen.

The MODFLOW-NWT solver was then set up for the model with a head tolerance for convergence, a maximum number of iterations out and a linearisation method was defined. The chosen head tolerance for convergence was set to 0.0001 m. The maximum number of iterations for the outer, nonlinear, problem was set to 100, meaning that 100 iterations was the maximum for solving the model for convergence. Linearisation method 2 was chosen which means that the χMD was used as matrix solver. The solver is adapted to MODFLOW-2005, that MODFLOW-NWT

is based on (Ibaraki et al., 2011). It was developed for more robustness, shorter execution time and to be more memory efficient.

4.3.3 Discretization

The DIS package was used for the discretization of the model. Discretization is made by defining a matrix in two dimensions or three dimensions if several layers are modeled. Since the rasters had a 10x10m resolution, the number of rows and columns were set to the dimensions of the rasters. A higher resolution could have been set but was disregarded in favour of decreased solver time and less memory issues. The 10x10 resolution was also set because of the limited resolution of rasters from SGU and the Land Survey, and considering the large area modelled.

The horizontal discretization was set with regards to the resolution of the topography raster to match the length and width of the modelled area in number of columns and rows.

The vertical discretization was set as a simplification of the stratigraphy. Seven layers was chosen in the model with the top set to the topography raster. A local reference point "gruvnollan" was defined for the layer divisions. The DIS package requires the bottom elevation for each of the layers. The layers and their partitioning elevations can be seen in Table 4.2. In layer 1 and 2, a layer thickness was set in contrast to a constant elevation. The thickness represents the more fractured and hydraulically permeable first hundred meters of the shallow bedrock. The following layers were set to constant elevation since it was assumed that the hydraulic conditions were not impacted by the surface fractures.

The input parameters for the DIS package was set to the model, the number of layers, number of rows and columns, the row and column width, the top of the model and the array of bottom levels for each layer respectively.

Table 4.2: Discretization stratigraphy. Reference point 281,03m (RH2000)

Layer name	**Start of layer**
Layer 0	topography
Layer 1	bedrock surface
Layer 2	50m below bedrock surface
Layer 3	100m below bedrock surface
Layer 4	320m below reference point, UM1988 bottom, UM2012 top
Layer 5	530m below reference point, UM2012 bottom
Layer 6	1000m below reference point, UM20XX bottom
Bottom of model	1500m below reference point, bottom of model

4.3.4 Boundaries, initial guess of head and recharge

To set the boundaries of the model the BAS package was used. A three-dimensional matrix named ibound was set up as can be seen in Figure 4.3. Cells corresponding with the no-flow raster were set to 0 for all layers to exclude areas that wouldn't impact the results. The cells representing lakes were set to -1 in all layers to represent constant head cells. Additional constant head boundaries were set to represent outflow from the catchment areas, since the model boundaries were not set to the catchment area geometry. These kinds of boundaries were set for parts of the northern, southern and western boundary. All other cells were set to 1, active cells.

The initial guess of ground water levels was set in a two dimensional matrix called strt to the topography. The specific water levels for each lake were assigned to match the constant head lake cells. In the BAS package, the ibound matrix and the strt matrix was added to the model.

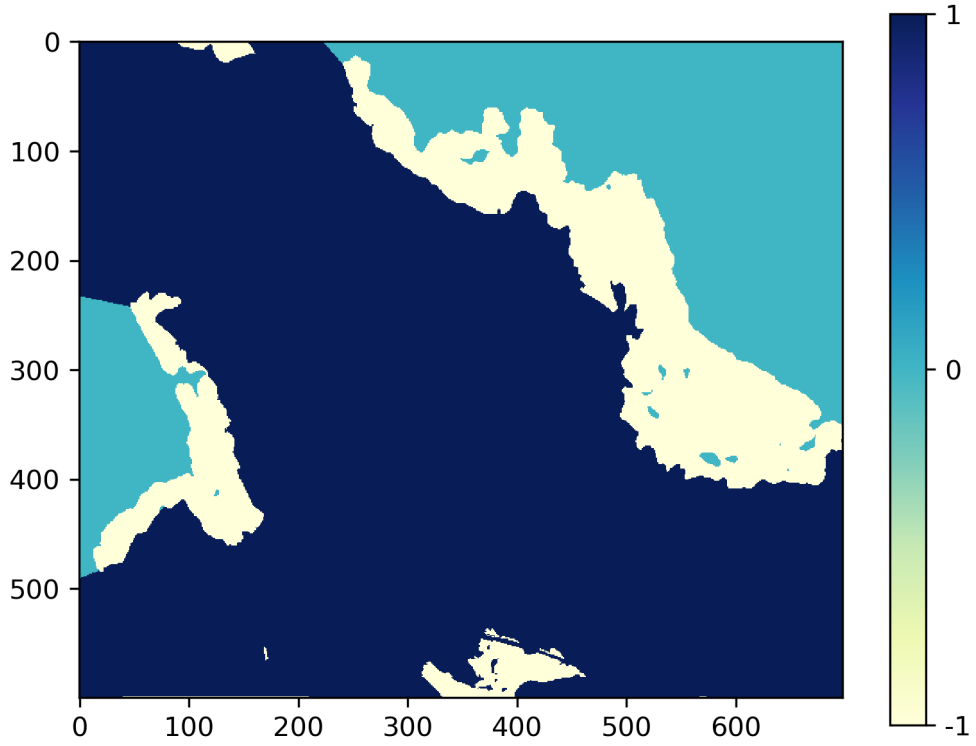

Figure 4.3: Hydraulic boundaries (1 = Active cell, 0 = No-flow cell, -1 = Constant head cell).

Recharge can be included by adding one representative value for the model, or with a recharge matrix or raster. For this project, a matrix was made called rech, with the same resolution as the discretization object. The recharge was assumed and set to different values depending on the cell location category. The categories were made considering areas with slopes larger than 5 degrees, wetland, lakes/rivers, no-flow areas and the open pit mine. Recharge were assigned in the model with the

priority order stated in Table 4.3 with decreasing priority. Additional recharge was added above the mine structures in the shape of circles, with diameters 900 m for the area of UM1988 and 2200 m for the area of UM2012. The recharge distribution is illustrated in Figure 4.4 with the values presented in Table 4.4.

The method for adding recharge in the package was set to number 3 which indicates that recharge is added in highest active cell in every layer. In this model, the alternative 1 could also be used which only adds the recharge to the top layer since the model has the same boundaries across every layer.

Table 4.3: Recharge definition

Category	**Location**	**Amount of recharge**
1	No-flow, lakes, rivers, peat	None
2	Slope > 5 %	Mid
3	General recharge	High
Solid red line	Surroundings of UM1988	High
Dashed red line	Surroundings of UM2012	High

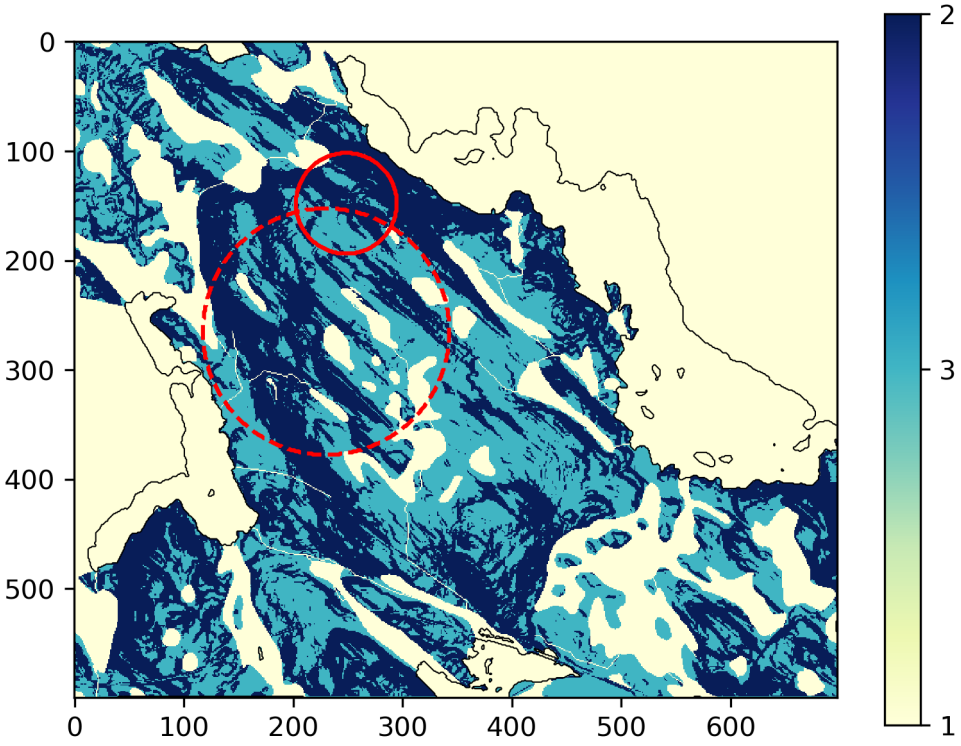

Figure 4.4: Recharge distribution based on categories and explanations in Table 4.3.

Table 4.4: Recharge values after calibration.

Recharge category	**Model 1**	**Model 2**	**Model 3**	**Unit**
1	None	None	None	mm/year
2	100	100	100	mm/year
3	180	180	180	mm/year
Area of UM1988	-	300	320	mm/year
Area of UM2012	-	-	240	mm/year
Average	110	113	129	mm/year

The amount of recharge can be calculated or estimated. Initially, recharge values were calculated using the water balance equation for hydrology as seen in Equation 4.1 as guidance. These calculated values were based on SMHI data of precipitation and evapotranspiration and an assumed surface runoff coefficient of 0.1 for forestry areas. Set recharge varies between the models due to it being a calibration parameter.

$$R = P - ET - RO \tag{4.1}$$

4.3.5 Hydraulic properties

To define hydraulic properties for flow between cells for the MODFLOW-NWT solver, the upper weighting package, UPW, was used. The method is similar to the LPF package which is not compatible with the solver of this model. The input for this package is the layer type, lists with the horizontal and vertical hydraulic conductivity and the ipackb=53. The layer type in soil was set to 1, since it was considered to be convertible rather than confined. All bedrock cells were set to layer type 0 for confined condition. Since it was a steady state model and not a transient model, the laywet input not used.

The hydraulic conductivity was set for each row, column and layer as presented in Table 4.5. Vertical hydraulic conductivity was set to be equal to the horizontal hydraulic conductivity. Ipackcb is a flag used for indicating if cell-by-cell budget should be printed in the budget or not. Hydraulic conductivities were assumed based on expert knowledge of hydrogeology in rock according to the data set DSOPEN for Model 1, and with regards to the field measurement data sets DS2009 and DS2022 for Model 2 and Model 3 respectively.

Table 4.5: Hydraulic conductivity in each layer after calibration.

Hydraulic conductivity	Model 1	Model 2	Model 3	Unit
hk0	1.0 E-5	8.0 E-6	9.6 E-6	m/s
hk1	5.0 E-7	2.5 E-7	6 E-7	m/s
hk2	2.5 E-8	1.5 E-8	9.0 E-8	m/s
hk3	2.5 E-9	1.5 E-8	9.0 E-8	m/s
hk4	2.5 E-9	6.0 E-9	9.0 E-9	m/s
hk5	2.5 E-9	6.0 E-9	8.0 E-9	m/s
hk6	2.5 E-9	6.0 E-9	8.0 E-10	m/s

4.3.6 Streams

To simulate the streams transporting water, the river package, RIV, was used. The river cells were used to drain stagnant water from the model, similar to the function of using the DRN package. The advantage of using the RIV package was that the water removed from the model by the river cells was categorized in the water budget file. The river cells were defined by the locations of the rivers in the SGU data and the addition of artificial rivers. The artificial rivers were added because of problems with water above surface level. The lakes, rivers and artificial rivers can be seen in Figure 4.5, where the artificial rivers are marked in orange.

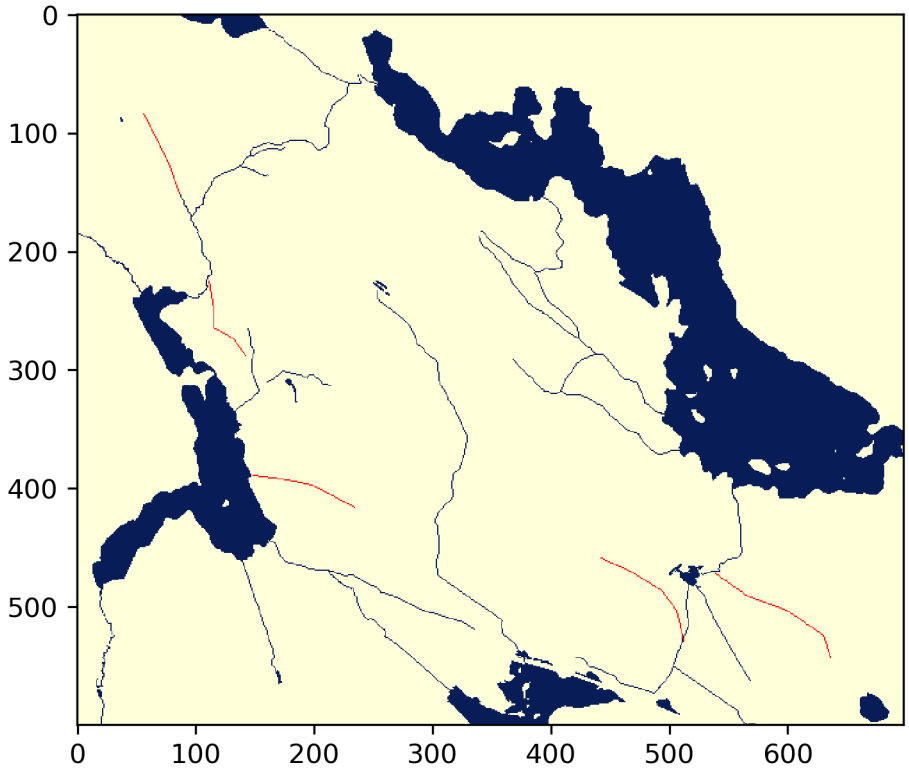

Figure 4.5: Lakes, rivers and artificial rivers. Artificial rivers marked in orange.

Input data for the RIV package was the location of the river cells in terms of discretization layer, row and column. The stage of the water table was also set for each cell as well as the conductance of the river bottom and the elevation of the river bottom (rbot).

When the head in neighboring cells are above the water level in the river (stage), groundwater gets drained and removed from the model. On the other hand, when the water level is below the river bottom, infinite amounts of water can be released into the model depending on the riverbed conductance. The sides of the rivers are defined as impermeable. The downside of this were that the rivers were not representative to reality. The stage was set differently depending on the soil depth to match the assumed resulting heads distribution in the area as well as minimal inflow in water budget. Small distance between stage and rbot was set to get the necessary drainage with the least amount of inflow into the model.

The rivers and streams were made into rasters from the "hl_riks' SGU map. River cells closer than 3 cells to a constant head boundary was removed to result in a more stable budget and reduce the amount of water flowing from a constant head boundary into a river cell.

Conductance in the RIV and DRN package are based on Darcy's law (Equation 4.2) and can be rewritten as Equation 4.3 (USGS, 2024). The conductance for the river cells and drain cells are therefore calculated with the expression in Equation 4.4.

$$Q = -K * A * \frac{h_1 - h_0}{X_1 - X_0} \tag{4.2}$$

$$Q = -C * (h_1 - h_0) \tag{4.3}$$

$$C = \frac{K * A}{(X_1 - X_0)} \tag{4.4}$$

Q=flow (L^3/T)
K=hydraulic conductivity (L/T)
A=area perpendicular to flow (L2)
h=head (L)
X=position at which head is measured (L)
C=conductance (L^2/T)

4.3.7 Drainage of the mines

The mines geometry was simplified to cylindrical shapes draining water from respective depths they were situated in. The OPM1966 and UM1988 were modelled as one cylinder with 200m diameter in the layers 0,1,2,3 (Figure 3.7). Water was actively drained from the surface down to -320m to simulate dry working environment.

The drain package (DRN) can be used to define head-dependent flux boundaries to simulate the draining of water. The input parameters used for DRN are the cells coordinates, the elevation of the drain and the conductance of the drain.

The elevation of ventilation shafts and the ramp was defined the same for each model. Elevation of ventilation shaft drains were set 0.1m from the cell bottom. The ramp has been modelled in two layers to simulate the gradient and inflow to ramp cells. The elevation for the top half of the ramp have been set 5m above the cell bottom in layer 3 and the other half, 5m from the top of the cell in layer 4.

Elevation of the drains have been set differently in each model during calibration for each mine. In Model 1, dry conditions were assumed throughout the mines and the elevation was set at the bottom of the respective mine or facility. This practice is a common way to model the largest possible area of influence. In Model 2, the elevation in the drain cells in the lowest layer of UM1988 were moved with an offset +170 m from the mine bottom. The drains were thereby only draining from the surface down to -120 m elevation. Model 3 drain elevations were set in the same manner as Model 1 and 2.

Conductance was calculated for Model 1 on the interface between the drain and the aquifer for each layer according to Equations 4.2, 4.3 and 4.4. For Model 2 and Model 3 the conductance was calibrated. Drains were set in each cell within the geometries of the mines, ventilation shafts and the ramp.

Other parts of the model that were individually calibrated was the elevation of drain cells and the conductance. The ramp was calibrated with lowering the conductance to 10 % of the calculated value.

4.3.8 Model run and post processing

The OC package was used for output control and for writing out stresses in the water budget file for a specified time step. Since the model, mf, was a steady state model, the end of the single time step was selected. Then, the necessary files from the packages was written in the model workspace using the mf.write_input function() and the model was run with the mf.run_model(). Post processing was then made by visualizing the results in plots.

4.3.9 Calibration

The groundwater levels were calibrated to match the datasets for each model. Before adding unknown stresses, the models were calibrated to reasonable hydraulic heads depending on the dataset. The hydraulic conductivity and recharge were adjusted.

4.3.9.1 Model 1 (M1)

The calibration for the unstressed model M1.0 aimed to result in a model that had little inflow into the model from constant head cells or river cells. Small lakes that gave an noticeable inflow in the water balance budget were removed from the model. The water level of the constant head cells was calibrated until the inflow constant head budget was reasonable. The stages of the river were calibrated in order to achieve the least amount into the water budget as possible. The rivers were calibrated with regards to soil depth. If the river cells had a soil depth smaller than 6m, stage and elevation of these cells were set to -3.9m respectively -4m below ground surface. If the soil depth were larger than 6m, the stage was set to -5.9m and elevation to 6m. Conductance of the rivers were calibrated and set to 1.

The Model 1.0 had problems with stagnant water in many areas. There were areas in the model where the natural rivers along with the other parameters did not manage to remove water from the surface regardless of the amount of recharge. This was solved by adding artificial rivers where water naturally would flow in wetlands and where groundwater could seep out as surface water on hillsides. The model was calibrated to have less than 1.5% heads over the surface.

The Model 1.1 and 1.2, were created as duplicates of Model 1.0 but with the addition of mine structures to simulate the draining in steps. No calibrations of groundwater levels and inflow were made in Model 1.1 and 1.2 since no data was available for these parameters. In Model 1.1, the UM1988 and the UM2012 together with a connecting ramp and three ventilation shafts were modelled with drain cells. In Model 1.2, the expansion, UM20XX, was modelled as an extension of UM2012 down to -1000 m from the surface. After running the respective models, results were obtained.

4.3.9.2 Model 2 (M2)

Model 2 was calibrated with DS2009, which contained data measured after the construction of UM1988 and the ramp. Model 2.0 was calibrated with respect to the groundwater levels in the wells available, and the measured inflow into the UM1988 and the ramp. The calibration consisted of varying the hydraulic conductivity and the recharge. The elevation of the drain cells in the UM1988 were also calibrated to match the measured inflow, meaning that the mine was not drained to the bottom. The ramp was calibrated to the measured inflow by changing the conductance. Results for Model 2.1 and Model 2.2 were obtained after adding the same mine structures as in Model 1.1 and Model 1.2 respectively.

4.3.9.3 Model 3 (M3)

Model 3 was calibrated to the dataset DS2022, with the largest amount of data, by varying the hydraulic conductivity and the recharge. The model was calibrated

with respect to groundwater level observations in newly drilled wells additional to the wells observed in DS2009. Measured inflow from the different structures of the mine were also available and taken into consideration when calibrating the Model 3.1.

The mine UM1988 were modelled as a pumping well using the well package (WEL) in Model 3 to represent the measured inflow in DS2022. The ramp was removed as drain cells in Model 3 and the inflow were instead modelled into UM1988 and UM2012. It was assumed to have little, to no impact on the results for area of influence since the inflow was calibrated accordingly. Results for Model 3.1 were obtained after calibration and the results for Model 3.2 after adding the UM20XX to the model.

5
Results

The results obtained for the model versions, presented conceptually in section 4.3, constitute the area of influence, the inflow for mine structures and the maximum drawdown in the centre of the Kankberg mine UM2012 and the potential expansion UM20XX. The results were obtained for the current scenario where OPM1966, UM1988, UM2012, the ramp and the ventilation shafts are constructed as well as for the scenario with the UM20XX expansion. A code example of Model 3.1 is included in Appendix A.8.

5.1 Area of influence

The area of influence was defined as the area where the simulated drawdown is larger than 0.3 m and the results are presented in Figure 5.1. The drawdown was evaluated as the difference between the current situation where OPM1966, UM1988, UM2012, the ramp and ventilation shafts were already existing, to the situation with the expansion of the UM20XX. The drawdown patterns are similar between the models as they spread out mostly in the northern and southern direction (Figure 5.1.D). The reason is that the lakes were set as constant head boundaries. Uneven shape of the area of influence is estimated to correlate to the hydraulic conductivity of the soil and the surfacing bedrock. The uneven shape can also be a result of topographic irregularities.

The results show differences between the models calibrated with different datasets. Model 1, the model with the data set containing only open-source data (DSOPEN) was simulating the smallest area of influence. The maximal drawdown is simulated to 5.0m, as seen in Figure 5.1.A. In the Figure, it can also be seen that large areas within the area of influence have a simulated drawdown of approximately 5m. The drawdown is therefore simulated to only affect the soil and the first few meters of bedrock.

The area of influence in Model 2, calibrated with DS2009, is simulated as a larger area, with maximum drawdown up to 27.5m generally affecting the area of the Kankberg mine and the immediate surroundings. The drawdown and the area of influence can be seen in Figure 5.1.B. No changes in groundwater levels are seen in the area of UM1988. The drawdown around the Kankberg mine were gradually increasing towards the middle of the mine location.

The last model, Model 3, calibrated with dataset DS2022, had an area of influence extending to the model boundaries, as seen in Figure 5.1.C. The maximal drawdown is simulated to 19.4m, and is mainly affecting the area near the Kankberg mine, and not directly above it. The result of calibrating groundwater levels to additional measurements have resulted in more realistic parameters in Model 3 compared to the other models. The predicted drawdown from adding the expansion was therefore less in Model 3 compared to Model 2 in this case.

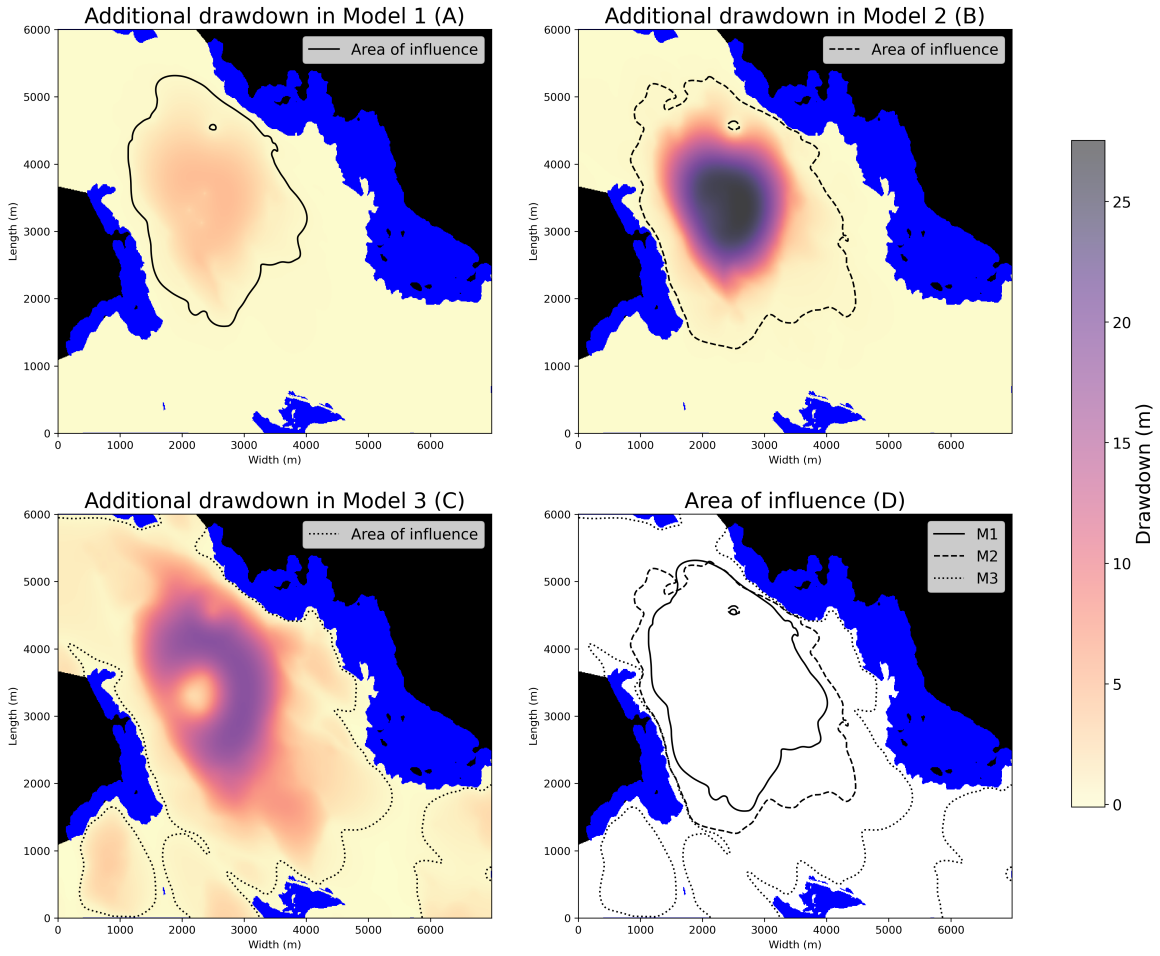

Figure 5.1: Figure A-C: Simulated area of influence and drawdown heatmaps for each model. Figure D: Area of influence for all models. Blue regions are constant head cells, and inactive cells are marked in black.

5.2 Drawdown at the Kankberg mine

The simulated groundwater tables in bedrock at the Kankberg mine are shown in Figure 5.2, where the mine is marked in grey. A figure showing the mine in full scale is presented in Appendix A.4 as well as a figure of the groundwater table without the impact of the expansion in A.5. The maximum drawdown from surface level, in the centre of the Kankberg mine and the expansion is presented in Table 5.1. The

results from Model 2.2 and Model 3.2 show similarities in the cone of depression above the mine. The drawdown heatmap of Model 3 5.1.C, presents the drawdown from the expansion compared to the current situation. A smaller additional drawdown is predicted at the Kankberg mine location, than the immediate surroundings. This implies that the expansion drains more water, and from a larger area in the deeper layer than the current mine.

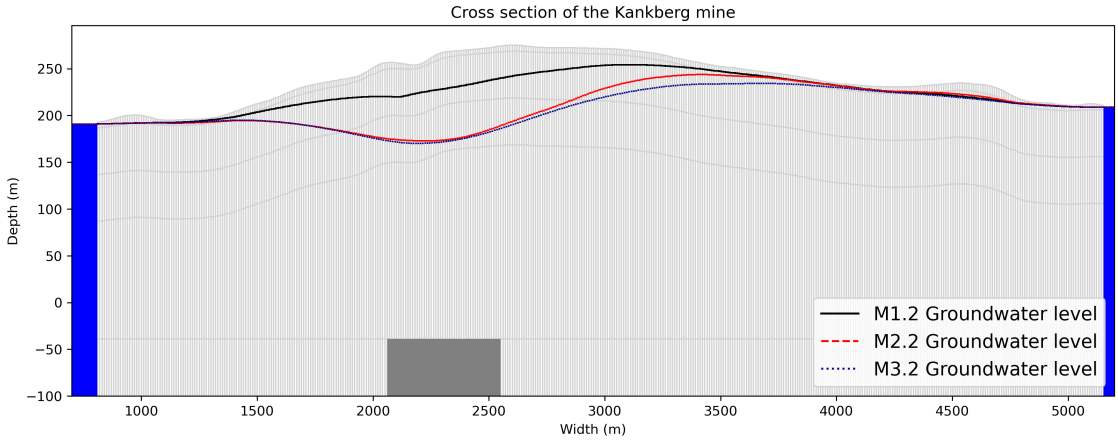

Figure 5.2: Simulated groundwater table in first bedrock layer for M1.2, M2.2 and M3.2. The Kankberg mine is seen in grey, and constant head cells in blue.

The drawdown from the surface level in the current situation is best predicted in Model 2 compared to field measurements as seen in 5.1. The drawdown is underestimated by 33m in Model 1 compared to measurements and overestimated with 24m in Model 3. Even so, the outcome of the predictions in Model 2 and Model 3 are very similar. The prediction in Model 1 can be stated to be underestimated since the groundwater levels are measured at a lower level in the current situation, before any expansion.

Table 5.1: Simulated and predicted drawdown in the centre of the Kankberg mine for the models. The measured value was obtained from Wladis (2022). Current structures include OPM1966, UM1988, UM2012, ramp and ventilation shafts.

Drawdown from surface level at the centre of the Kankberg mine	**M1.2**	**M2.2**	**M3.2**	**Measured**	**Unit**
Current structures	35	68	92	approx. 70	m
Prediction of the expansion	39	94	9 6	-	m

5.2.1 RMSE

An error was calculated between the observed groundwater levels in wells and the simulated groundwater levels for Model 2 and Model 3. In Model 2, the well KA0501 was identified as an outlier, potentially crossing structures such as another exploitation drift, that were disregarded in the model. In Model 2, the root mean square

error (RMSE) of the groundwater levels was 2.7m, after the outlier was removed. The distribution of the error can be seen in Appendix as Figure A.6. In Model 3, the RMSE of groundwater levels were 7.6m, and no wells were removed. The error distribution can be seen in Appendix as Figure A.7. This means that the drawdown in Model 2 have a better chance to result in correct predictions than Model 3.

5.3 Inflow

The results for inflow predictions is presented in Table 5.2. Generally, Model 1 and Model 2 underestimated the results for the current structures (UM1966, UM1988, UM2012, ramp, ventilation shafts) compared to the measured inflow.
The reason for this could be due to underestimated hydraulic conductivity in the UM2012 and UM1988 layers and an underestimated recharge. In other words, the bedrock in these models could have been assumed to be less fractured than the measurements indicated. For the current structures, the inflow was calibrated to the measured values by finding an optimum for hydraulic conductivity and recharge. The most accurate model in terms of inflow, is Model 3 which has the most data, and the second best is Model 2 which underestimated the inflow of the current structures by 39%.

Table 5.2: Simulated inflow in m^3/h for mine structures from the models. Measured inflow was obtained from Wladis (2022). *results collected for current structures from model versions M1.1, M2.1 and M3.1, ** results collected from versions M1.2, M2.2 and M3.2, *** calculated difference

Mine structure & model version	**M1**	**M2**	**M3**	**Measured**	**Unit**
UM1966, UM1988, UM2012, ramp, vs*	31.5	57.7	94.2	95.3	m^3/h
UM20XX***	16.4	41.3	48.6	-	m^3/h
*Total***	*47.9*	*99.0*	*142.8*	-	m^3/h

The predictions for the inflow associated with the expansion UM20XX varied between the models. Model 1, based on open-source data, predicted a inflow flow for UM20XX 60% smaller than Model 2, calibrated with DS2009. Model 1 also predicted a 66 % smaller inflow flow than Model 3, calibrated with DS2009 with DS2022. The accuracy of the simulated inflow can be considered to correlate to the accuracy of the simulation of the current structures. Noteworthy is that the hydraulic conductivity was set equally in the Kankberg mine layer as the expansion layer for all models, not taking the conceptually decreasing hydraulic conductivity in consideration.

The difference in result is larger comparing Model 1 to Model 2 and Model 3, than comparing Model 2 to Model 3. The differences are therefore larger between only using open-source data (DSOPEN) and using field measurements (DS2009 or DS2022), than between using different quality or quantity of field measurements. The added data of groundwater levels in wells closer to Kankberg mine and the measured inflow

in the current structures from DS2022 resulted in a more realistic prediction for the total inflow of the mines. The predictions for the expansions were similar between Model 2 and 3 but no correlation for the simulated inflow can be established based on the datasets in the results.

6
Discussion

6.1 Value of data

The importance of the quality of data can be evaluated based on the result from the models. Clear differences in area of influence, drawdown and inflow was identified between the open-source data model and the other two models calibrated with field measurements.

6.1.1 Groundwater levels

When using only open-source data with no measured groundwater levels, the accuracy of the results of the model becomes uncertain. The main problem is the lack of a comparable parameter, which makes validation of groundwater levels based only on assumptions. In this study, the open-source model were underestimating groundwater drawdown. When stress is applied to an open-source data model, the results can either be overestimated or underestimated depending on the situation and it can be difficult to evaluate. Each parameter can be calibrated into a balanced situation with unreasonable parameters and every parameter is considered an "known unknown". Meaning that all parameters are considered as uncertain. When all parameters are uncertain, the question is if the model itself can be considered certain.

Measured groundwater levels is an easy way of adding a known parameter into a model. The main uncertainty with measured groundwater levels in bedrock is the risk of a well being located in a local fracture, not necessarily representing the modelled area. Measurements from several wells better ensures that some wells are located in the fracture network and therefore are representative for the study.

In some cases, the open-source data could include private drilled wells for drinking water or geothermal heat pumps within the modelled area and the assumed area of influence. In these cases, one or several measurements could be included in the modelling, leading to a decreased need for additional measurements. In the case of available private wells in the SGU wells archive a larger focus could be pointed to spending money on other things than drilling wells.

It was found in the study in Kankberg, that the most important data in the modelling of Model 2 was the measured groundwater levels. Using the groundwater levels

made it possible to calculate an error using the RMSE equation (Equation 2.5). The RMSE gave a measurement of how good the prediction was, which was not possible in Model 1, with only open-source data. In Model 2, an outlier was observed in the observation well KA0501. The measurement was significantly higher than the simulated head and the assumption was made that it probably is drilled into a local fracture, disconnected to the fracture network. If the measurements was kept, the calibration would have taken a local condition into consideration for the entire study area. The measurement was removed, and therefore a rather small RMSE, 2.7m, was calculated. With the outlier present, further calibration would have slightly altered the parameters in Model 2, probably resulting in a higher RMSE.

In Model 3, the groundwater levels were, again, the most important data. The RMSE were calculated larger than in Model 2, giving an indication of further calibration possibilities of Model 3. The RMSE was calculated to 7.6m, but at the Kankberg mine it occurred a difference up to 13m between the model heads and the observed measured heads. In Model 3, a higher number of groundwater level measurements were included, which gives opportunity for higher accuracy in calibration. To achieve a higher accuracy, a more time consuming calibration process is needed. It might also be necessary to adjust parameters and processes in a more complex way, e.g. introducing local variations of hydraulic conductivity with depth. The variations in hydraulic conductivity could represent the bedrock types within the model area and include local conditions. For example, in the permit application process from 2022, it was found that the bedrock containing the ore had lower hydraulic conductivity than the surrounding bedrock, which could be represented in the model with this application.

In the calibration process, the wells N. Åkulla and S. Åkulla were important. The two wells were located approximately 600-900m from the Kankberg mine and 900-2000m from old Kankberg mine. The groundwater levels were important both in terms of calibrating a representative hydraulic conductivity and a representative area of influence due to their location. When planning where to drill wells for field measurements, it is important to consider the distance to the modelled structure. Wells close to the structure showcases the cone of depression, but in order to capture the area of influence, wells are also needed further away. In this study, no wells at a far distance were available and due to that, the predicted area of influence was not validated. The predicted area of influence varied between the models, but because no validation was possible, it is uncertain which model performed the best result. Because of modelling underground structures, wells located right by the structure of interest can also be helpful to make validating measurements on the maximum drawdown after construction.

6.1.2 Hydraulic conductivity

The drawdown from surface level were dependent on the decrease of the hydraulic conductivities with depth in the model. Model 1 with open-source data were under-

estimating drawdown and inflow, which implies that the hydraulic conductivity also were underestimated, at least in some layers. Conceptual understanding of decreasing hydraulic conductivities with depth is important but is not necessarily enough to create an accurate model.

The similarities in drawdown between Model 2 and Model 3, see Figure 5.2, were probably caused by similar hydraulic conductivities in the deeper layers. The hydraulic conductivity in deep layers could have been more included in calibration to match the conceptual model. The mine inflow and the drawdown are posing a risk of being overestimated due to the overestimated hydraulic conductivity.

Field measurements of hydraulic conductivity were interesting as guidance in numerical modelling, but not always very easy to use. In the dataset from 2022, DS2022, many hydraulic conductivities were evaluated from pumping tests but was mainly used as a guiding range of values for respective modelled layer. The hydraulic conductivity was instead used as a calibration parameter to satisfy measurements of groundwater levels and mine inflow. Since an average value was used for each layer, it was not possible to use all the evaluations for a more local based assignment of hydraulic conductivity. The risk of using pumping tests in groundwater modelling in bedrock are that evaluated conductivity could be locally accurate rather than representative for the entire modelled area.

Evaluations of hydraulic conductivity at larger depths of the bedrock could have been useful for guidance. Evaluations were made in the exploration drift at level 430m in a set of core drillings in DS2009. These were not considered reliable because of them not being drilled for hydrogeological purposes, but rather to find the direction of the ore. If tests in the exploration drift was made for hydrogeological evaluation with better representative values, then they could have been used in the modelling.

6.1.3 Measured inflow

The results showed that the inflow was underestimated in both Model 1 and Model 2 in comparison to the measured inflow in DS2022. The predictions of the total inflow with the expansion can therefore be seen as underestimations, in addition to that, the simulated inflow flow also differs to a large extent between the models.

The recharge and hydraulic conductivity were calibrated to fit the measured inflow in Model 3, implying that either recharge or hydraulic conductivity, or both, are underestimated in the previous models. Model 2 were also calibrated to measured inflow in old Kankberg mine (OPM1966 and UM1988), but still gave underestimations of the inflow in the Kankberg mine. The cone of depression in Model 2 and Model 3 are similar, but the total inflow flow in Model 2 is modelled 30% lower than in Model 3.

The inflow can be seen as an unpredictable simulated parameter that has a high value in terms of data collection. If possible, it would be more valuable to measure inflow in the exploration drift, rather than evaluating the hydraulic conductivity with pumping tests or pressure build up tests.

6.2 Model method and calibration method

To be able to conduct the project, a continuum model was utilized as a representation of the model area containing fractured bedrock. The representation was necessary to use the numerical modelling method MODFLOW. The consequences of this were less level of detail in terms of local hydraulic conductivity in the fractures. Hydraulic conductivity could have been set locally to different values for each layers but because of processing time and the difficulty of calibrating the model, an average values were used instead. The prediction of the areas where hydraulic conductivity locally differed would be outside the scope of the project.

A variation in hydraulic conductivity based on local conditions, like different bedrock types, would make the model more complex. The application would include several types of bedrock in each layer, making it possible to capture the variation in hydraulic properties with more detail. The consequence of several set hydraulic conductivites within each layer is a more complex calibration and evaluation process. The model could potentially be better with local variation in hydraulic conductivity, but additional data of bedrock type or fracture systems would be necessary. Although, it's likely that the model would not significantly improve to justify the additional costs for evaluation and modelling. In this case, possible improvement of the results could have been achieved by knowing the three dimensional spatial distribution of different lithological units. The hydraulic conductivity could have been locally altered to simulate more accurate groundwater levels for the mine structures. The addition of more data would have made the evaluation of the results and value of each data set more complex.

In the datasets, some indication was found that large measured inflow was caused by a ventilation shaft being hydraulically connected to an old, water filled exploration drift. Within the scope of the project it was not possible to model a correct representation of this process. Since a stable flow was observed, the impact of modelling the water filled exploration drift was not of interest. If the expansion of the Kankberg mine instead was modelled for the scenario above the existing mine, then it might have been necessary to include the structure in the model. The drifts of the expanded mine would probably intersect and cross the exploration drift causing larger inflows.

The model was set up as a steady state model with input parameters representative for a yearly average. Seasonal variations were therefore excluded from the evaluations. If the model would have been a transient model, variations in recharge would be included, resulting in smaller areas of influence when recharge is high and larger

areas when recharge is low. The model therefore does not represent a specific time of the year, but rather an average yearly predicted inflow. In terms of permit application process, it needs to be noted that the seasonal variations are excluded. During snow melting, a possible scenario could be increased recharge and increased inflow from the shallow mines. When considering a maximum flow in the legal requirements in the environmental permit, it needs to be noted that the modelled results are not representative as a maximum inflow of the seasonal variation.

6.2.1 Discretization and boundaries

In the case study area, rock outcrops were disregarded in the modelling. To ensure model stability and convergence, a threshold of the soil depth was set to 3m by lowering the bedrock in areas where the condition was not met. The consequences of the threshold could have impacted the results by increasing the area of influence, since the hydraulic conductivity was larger in the soil than in the bedrock. The groundwater levels were therefore observed in the first bedrock layer.

The shape of the modelled area was selected as a rectangle rather than be based on catchment area, mainly because of no available shape file for clipping. The consequences of the rectangular shape of the area were the need for constant head boundaries to simulate the groundwater flow in and out of the area within the catchment. This is a common practice when modelling and is assumed to not impact the results significantly. The advantages of using a smaller area to model rather than a catchment area is less processing time. Results from a full catchment area model could match those from a cropped area if hydrogeological processes are properly considered.

Due to issues with too much water in the model, stagnant bodies of water were present in all models. River cells was used to simulate streams where surface water and groundwater is transported within the modelled area. The stagnant water was thus removed with the river cells.
The issue with using river cells is that they add infinite amount of water when the simulated head in the cell is below the river bottom. The addition of water from the streams diverges from the conceptual model. Calibration was therefore made to find an optimal river bottom elevation and conductance. The river cells were calibrated to act as a transporter of water without adding water to the model. The error due to inflow from river cells were less than 0.7% of the total water budget into the model which was assumed as acceptable.

Artificial streams were also added which makes the model less reliable. The aim was to simulate flows within the wetlands and to cope with stagnant water in the foot of the western hillside of Kankberg next to Stavträsket. These were calibrated simultaneously as the streams from the SGU shape file and was therefore included in the evaluation of the river inflow.

6.2.2 Parameters

The recharge parameter was one of the most uncertain parameters. It was modelled based on recharge in soil, which makes the recharge to the bedrock dependent on vertical hydraulic conductivity. Categorization of recharge areas was used to distribute water and minimize areas with otherwise stagnant water. The areas were determined based on conceptual knowledge of infiltration in wetlands and slopes. The recharge was generally underestimated in the respective models for the categorization. In the case study area, the recharge in glacial till was estimated to 300-375 mm/year. In the model, the average recharge when considering slopes and wetlands resulted in 110, 113 and 129 mm/year for Model 1, 2 and 3 respectively. The reason for the relatively low recharge values in soil was because of the stagnant water on the surface. The low recharge was also intentionally set to minimize the removed water with rivers or other processes. The underestimation of average recharge could have impacted the results in underestimations of inflow and overestimated areas of influence. When the models were calibrated to the measured inflow in the deeper layers, vertical hydraulic conductivity could have been overestimated to compensate for the low recharge at the surface.

When setting up Model 2 and Model 3, larger recharge was added by the UM1988 and UM2012 to better represent the estimated recharge in the area of 300-375mm/year. The recharge was used to calibrate the model to the measured groundwater head and mine inflow. The local change of recharge differed from the conceptual model which was based on variation in recharge based on soil type and slope angle. The outcome of adding the recharge was a cone of depressions that better matched the measured groundwater levels and the measured inflow in the mine structures. The recharge of 300 mm/year would ideally been added on the entire case study area to give the most representative results.

The conductance was dependent of the hydraulic conductivity, causing more water to drain when overestimated. The conductance was calculated and not calibrated during the modelling because of the uncertainty of the parameter.

6.2.3 Stresses from mine structures

For the mines without measured inflow, a drainage elevation was set to the bottom of each mine to simulate a worst-case scenario. Although, after the calibration, it was found that not all mine structures were drained to the bottom level. This corresponds quite well with the reality where it has been observed groundwater inflow in the walls of the structures. It was also found that the simulated groundwater heads followed the conceptualisation of groundwater around a draining tunnel by Gustafson (2012) as seen in Figure 5.2.

The mine UM1988 was modelled in different ways between the models. In Model 2, the drain elevation was set higher than the mine bottom, which implies that a worst-case scenario is not considered, or that the mine in the conceptual model

is not drained to the bottom. In reality though, seepage faces are present where flow is seeping into the mine, meaning that the groundwater levels are not in fact completely drain to the mine bottom. It was considered reasonable to change the elevation due to the measured inflow and the groundwater level measurements. In Model 3, the UM1988 was modelled as a well, since a stable measured inflow were known. Using a well is a simplification but were necessary due to time constrains with calibration.

The ventilation shafts were modelled as single cells, meaning that each ventilation shaft had the geometry 10x10m. This does not correspond to reality, but was a consequence due to grid spacing limitations. The impact of the overestimated ventilation shafts were not evaluated since the calibration was conducted by combining the ventilation shafts with the UM2012.

6.3 Bias in modelling

Because of the limited time, the work was distributed in the project. The model development and the compiling of the calibration data were mainly conducted separately. Some information was passed on to the modeler creating some bias. Ethically, the study is not posing any risk of bias, since the authors have no beforehand connection to the company Boliden Minerals AB, and no economical compensation is involved.

6.4 Further research

The study focused on evaluating the impact of data in numerical groundwater modelling in terms of modelled output. The results were evaluated based on the accuracy of the results for the current Kankberg mine and the downward expansion. For the current Kankberg mine, field measures on mine inflow were available making it possible to compare simulations to an observation. In the case of the expansion, simulated predictions were compared.

A suggested further study would be to use the result as input in a value of information analysis (VOIA) (Freeze et al., 1992). In the VOIA, costs for the permit application process could be included and evaluated to costs and risks regarding the permit process and legal fulfillment of the permit. The costs included could consist of costs of conducting field measurements compared to the risk of inaccurate assessment. Inaccurate assessment could result in requirements that are unreasonable in terms of fulfillment in the operating stage. Consequences to unreasonable requirements can lead to both costly actions or the risk of violating the permit. Violating an environmental permit could lead to sanctions such as fees and penalties, prison time and losing the permit, meaning that the permit application needs to be remade.

It would also be interested to conduct a similar study for an open pit mine in both a transient model and a steady state model. The transient model would simulate the seasonal variations in groundwater recharge resulting in maximum and minimum flows throughout an average year. The results would then be compared to the steady state model and evaluated in terms of model accuracy and value information in regard to an environmental permit application. The legal requirements of fulfillment are usually set as a maximum flow of groundwater into the operating mine.

Conducting the same study in MODFLOW-6 and compare the results to the study made with MODFLOW-NWT would be interesting in terms of model accuracy. In MODFLOW-6 an option is available to categorize and name the drain cells using the "boundnames" as input parameter. The calibration process could therefore be improved, possibly resulting in more accurate simulations for the Kankberg mine and the predictions for the expansion. The results using MODFLOW-6 could be compared with the results from this study, using MODFLOW-NWT. Additional packages for local grid refinement or unstructured grid refinement could be used and evaluated if they simulate results more reliable in a permit application process or not.

7
Conclusion

The outcome of the project were three numerical models calibrated with three different levels of site-specific data. Compared to the current situation, the open-source based model, Model 1, resulted in underestimated groundwater drawdown and inflow. Model 2, calibrated with measured groundwater levels, hydraulic conductivity and inflow from 2009, resulted in reasonable groundwater levels and drawdown patterns, but underestimated inflow in the current mine structures. Model 3 were calibrated with data from 2022, and were found to be overestimating drawdown, probably because of time constrains in calibration.

The main conclusions of this study are as follows:

- The predicted impact of the expansion is stated as underestimated in the open-source data model. Drawdown and mine inflow predictions were underestimated compared to measured values with current mine structures.
- The predictions of the area of influence and drawdown pattern due to the expanded mine were similar for the models calibrated to field measurements.
- In the predictions of mine inflow, larger differences were observed and is assumed to be dependent on the hydraulic conductivity.
- The most important type of data was found to be groundwater level measurements, since the measurements makes validation of the model results possible.
- The wells should be placed with intention. Wells are needed close to the mine to capture the cone of depression and the maximum drawdown. Wells are also valuable at a larger distance for validation of the area of influence.
- The measured inflow in the underground structures were the second most important data for calibrating a reliable model. Inflow into the underground structures is an unpredictable parameter in analytical evaluation, which makes it valuable to measure and include in the data collection.
- Hydraulic conductivity measurements were seen as guiding values for the numerical modelling, because of the large range in the field measurements. The hydraulic conductivity was altered in calibration, and estimated theoretically at the depth of the Kankberg mine. Additional hydraulic conductivity measurements could be valuable in the underground construction depth for better guiding values.

The study gives insight in the environmental problems regarding groundwater in relation to mining operations. It was found that some field measurements are more valuable than others in an environmental permit application including numerical modelling. Therefore, it is not likely to be able to create a reliable numerical groundwater model with only open-source data without any field measurements.

Bibliography

Anderson, M. P., Woessner, W. W., and Hunt, R. J. (2015). *Applied Groundwater Modeling - Simulation of Flow and Advective Transport*. Elseiver, 2nd edition.

Aramendia, E., Brockway, P. E., Taylor, P. G., and Norman, J. (2023). Global energy consumption of the mineral mining industry: Exploring the historical perspective and future pathways to 2060. *Global Environmental Change*, 83.

Bakker, M., Post, V., Langevin, C. D., Hughes, J. D., White, J. T., Starn, J. J., and Fienen, M. N. (2016). Scripting MODFLOW Model Development Using Python and FloPy. *Groundwater*, 54(5):733–739.

Chiang, W.-H. and Kinzelbach, W. (1991). Processing Modflow A SIMULATION SYSTEM FOR MODELING GROUNDWATER FLOW AND POLLUTION. Technical report.

Eniro (2024). Sok i kartan.

Fetter, C. (2014). *Applied hydrogeology*. Pearson Education Limited, Harlow, fourth edition.

Freeze, R. A., James, B., Massmann, J., Sperling, T., and Smith, L. (1992). Hydrogeological Decision Analysis: 4. The Concept of Data Worth and Its Use in the Development of Site Investigation Strategies. *Groundwater*, 30(4):574–588.

Grinevskii, S. O. (2014). The effect of topography on the formation of groundwater recharge. *Moscow University Geology Bulletin*, 69(1):47–52.

Gustafson, G. (2012). *Hydrogeology for Rock Engineers*. BeFo - Rock Engineering Research Foundation.

Harbaugh, A. W. (2005). MODFLOW-2005, The U.S. Geological Survey Modular Ground-Water Model-the Ground-Water Flow Process. In *Book 6. Modeling techniques*. Reston, Virginia.

Hölting, B. and Coldewey, W. G. (2019). *Hydrogeology*. Springer Nature, Berlin, Germany.

Ibaraki, M., Panday, S., Niswonger, R. G., and Langevin, C. D. (2011). Improvement of performance and applicability of MODFLOW-2005: new NWT solver and χMD matrix solver package. Technical report.

Jain, R. K., Cui, Z., and Domen, J. K. (2016). Environmental Impacts of Mining. *Environmental Impact of Mining and Mineral Processing*, pages 53–157.

Kathol, B. and Weihed, P. (2005). Ba57 Description of regional geological and geophysical maps of the Skellefte District and surrounding areas. Technical report, Svergies geologiska undersökning.

Lewis, J., Sjöström, J., Höök, M., and Sundström, B. (2013). The Swedish model for groundwater policy: legal foundations, decision-making and practical application. *Hydrogeology Journal*, 21(4):751–760.

Michanek, G. and Zetterberg, C. (2017). *Den Svenska Miljörätten*. Iustus Förlag AB, Uppsala, 4:2 edition.

Moran, C. J., Lodhia, S., Kunz, N. C., and Huisingh, D. (2014). Sustainability in mining, minerals and energy: new processes, pathways and human interactions for a cautiously optimistic future. *Journal of Cleaner Production*, 84(1):1–15.

Ofterdinger, U., Macdonald, A. M., Comte, J. C., and Young, M. E. (2019). Groundwater in fractured bedrock environments: Managing catchment and subsurface resources – an introduction. In *Geological Society Special Publication*, volume 479, pages 1–9. Geological Society of London.

Olofsson, B. (1994). Flow Of Groundwater From Soil To Crystalline Rock. *Applied Hydrogeology*, 2(3):71–83.

Pujades, E. and Jurado, A. (2021). Groundwater-related aspects during the development of deep excavations below the water table: A short review. *Underground Space*, 6(1):35–45.

Rodhe, A. and Bockgård, N. (2006). Groundwater recharge in a hard rock aquifer: A conceptual model including surface-loading effects. *Journal of Hydrology*, 330(3-4):389–401.

Rova, J. and Paulsson, K. (2015). Restaurering av en värdefull naturtyp MYREN. Technical report, Länsstyrelsen.

SFS 1998:808 (2024). .

SGU (2016). Vägledning för prövning av gruvverksamhet SGU-rapport 2016:23. Technical report, Sveriges geologiska undersökning.

SLU (2024). Sök digitala kartor och geodata.

SMHI and Havs- och vattenmyndigheten (2024). Modelldata per avrinningsområde - Vattenwebb Arkiv.

Söderholm, P. and Svahn, N. (2015). Mining, regional development and benefit-sharing in developed countries. *Resources Policy*, 45:78–91.

SOU (2022). *En tryggad försörjning av metaller och mineral - Betänkande av Utredningen om en hållbar försörjning av innovationskritiska metaller och mineral (SOU 2022:56)*. Stockholm.

Statens rad for karnavfallsfragor (KASAM) (2005). Karnavfall - barriarerna, biosfaren och samhallet SOU2005:47. Technical report, Statens offentliga utredningar (SOU), Stockholm.

USGS (2024). Online Guide to MODFLOW - Frequently Asked Questions.

Vatteninformationssystem Sverige (VISS) (2024). Vattenkartan.

Voigt, B. and Bradley, J. (2020). Boliden Summary Report Kankberg.

Wessman, H., Salmi, O., Kohl, J., Kinnunen, P., Saarivuori, E., and Mroueh, U. M. (2014). Water and society: mutual challenges for eco-efficient and socially acceptable mining in Finland. *Journal of Cleaner Production*, 84(1):289–298.

Winston, R. (2019). ModelMuse Version 4: A Graphical User Interface for MODFLOW 6. Technical report, Reston, Virginia.

Wladis, D. (2009). PM Hydrogeologi - Kankbergsgruvan.

Wladis, D. (2022). PM HYDROGEOLOGI-KANKBERG.

Yeh, H. F., Lee, C. H., Hsu, K. C., and Chang, P. H. (2009). GIS for the assessment of the groundwater recharge potential zone. *Environmental Geology*, 58(1):185–195.

A

Appendix

A.1 Products downloaded from SLU "GET"

Authority	**Product name**
Lantmäteriet	Höjddata, grid 2+ 2019 CLIP (tif) *Elevation grid 2+*
SGU	Jorddjupsmodell latest (shp, tif) *Depth of earth*
SGU	Berggrund 1:50 000 - 1:250 000 (tif) *Bedrock*
SGU	Jordarter 1: 25 000 - 1:100 000 latest (shp) *Quarternary deposites*
SGU	Brunnar latest (shp) *Wells*
Lantmäteriet	GSD-Fastighetskartan vektor / Hydrografi latest *Property map Hydrography*

A.2 Files used from respective product

Product	**Files used**
Elevation grid 2+	hojddata2_mosaik
Depth of earth	jorddjup_10x10
Bedrock	berggrund_50_250k_geo_enh_y
Quartenary deposits	jordarter_25_100k_jg2_north
Wells	bark
Property map Hydrography	hl
Property map Hydrography	mv

A.3 Measured groundwater levels at Kankberg for wells KA0503-0505 from Wladis (2022).

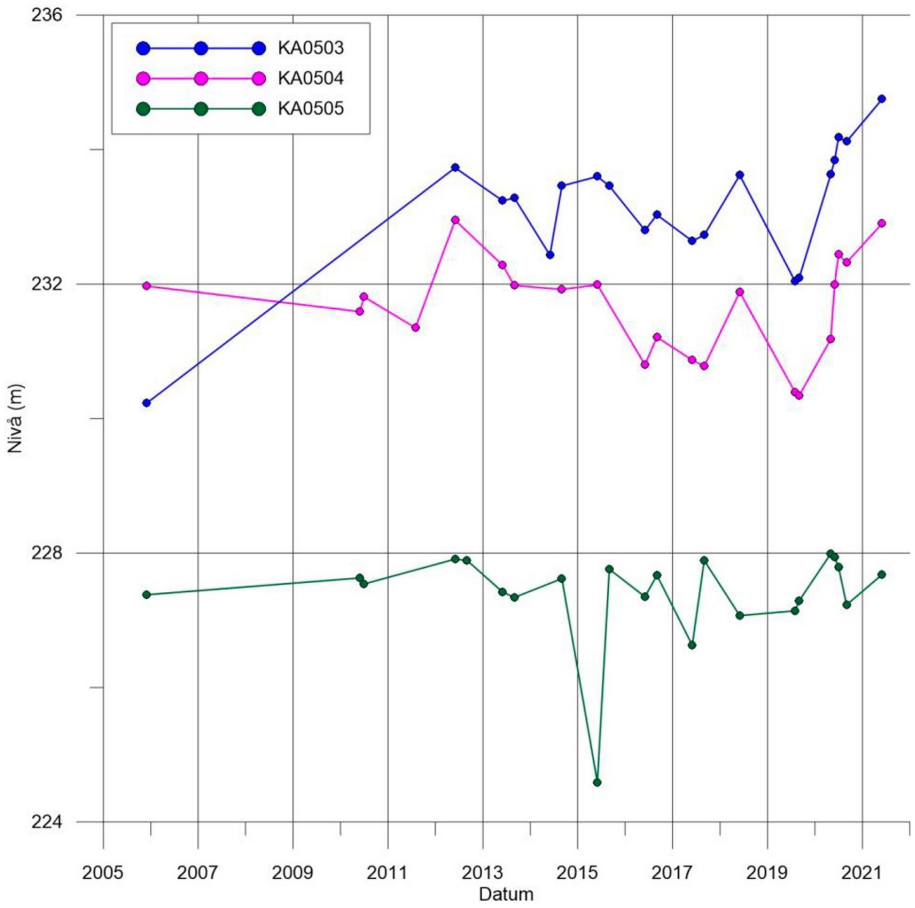

A.4 Simulated groundwater tables, at the Kankberg mine (marked in grey).

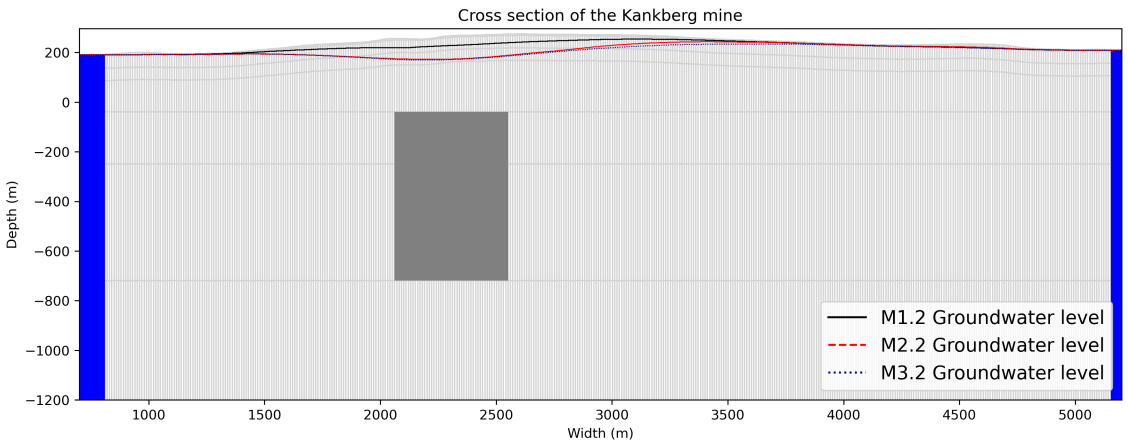

A.5 Simulated groundwater tables without impact of the expansion, at the Kankberg mine (marked in grey).

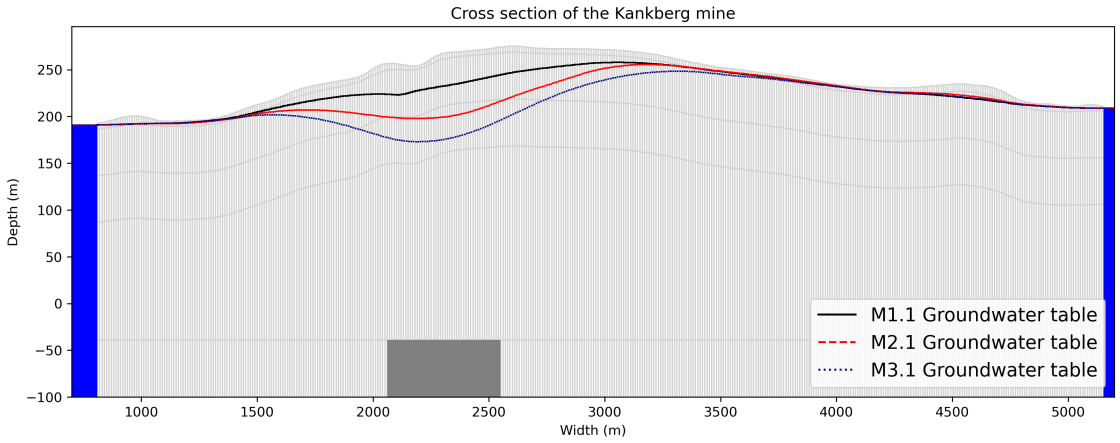

A.6 Error distribution in Model 2. Observed groundwater levels plotted to the simulated groundwater levels.

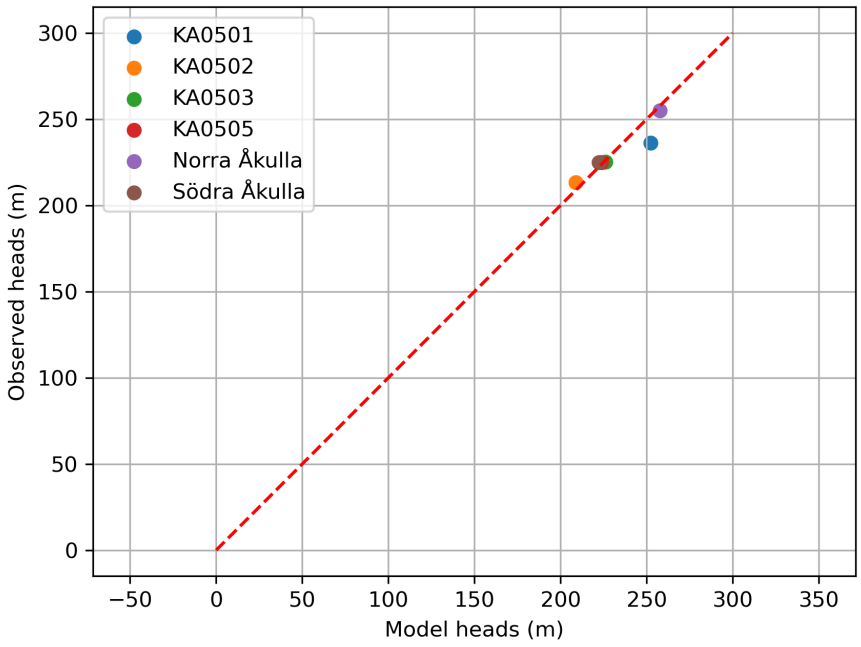

A.7 Error distribution in Model 3. Observed groundwater levels plotted to the simulated groundwater levels.

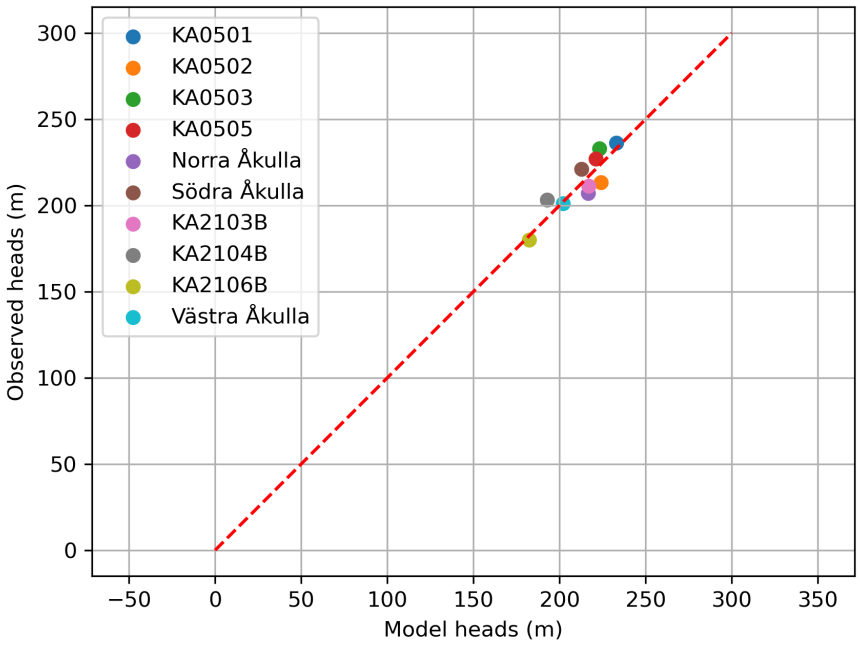

Figure A.1: Error distribution in Model 3. Observed groundwater levels plotted against the simulated groundwater levels.

A.8 Example code for Model 3.1

Kankberg groundwater model - Model 3.1

This version of the model is simulating the current mine structures near the Kankberg mine, Skellefteå. The addition of the expansion could be modelled if needed.

In [1]:
```
import flopy
import numpy as np
import os
import matplotlib.pyplot as plt
import matplotlib.gridspec as gridspec
import rasterio
import rasterio.mask as riomask
import flopy.utils.binaryfile as bf
```

Geospatial analysis

Load rasters

In [2]:
```
# Topography
path_topography= 'Kankberg_Data/topography.tif'
ds_top = rasterio.open(path_topography)
top= ds_top.read(1)

# Bedrock
path_bedrock = 'Kankberg_Data/bedrock.tif'
ds_bed = rasterio.open(path_bedrock)
bed = ds_bed.read(1)

# Lakes
path_lake = 'Kankberg_Data/lakes.tif'
ds_lake = rasterio.open(path_lake)
lake = ds_lake.read(1)

# Rivers (bäckar)
path_river = 'Kankberg_Data/rivers.tif'
ds_river = rasterio.open(path_river)
river = ds_river.read(1)

# Peat (torv/våtmarksområden)
path_peat = 'Kankberg_Data/peat.tif'
ds_peat = rasterio.open(path_peat)
peat = ds_peat.read(1)

# No flow boundaries
path_noflow = 'Kankberg_Data/noflow.tif'
ds_noflow = rasterio.open(path_noflow)
noflow = ds_noflow.read(1)

# Slope
path_slope = 'Kankberg_Data/slope_percent.tif'
ds_slope = rasterio.open(path_slope)
slope = ds_slope.read(1)

# Old underground mine & underground mine
path_um = 'Kankberg_Data/UM_OUM.tif'
ds_um = rasterio.open(path_um)
um = ds_um.read(1)

# Ventilation shafts
path_vs = 'Kankberg_Data/vs.tif'
ds_vs = rasterio.open(path_vs)
vs = ds_vs.read(1)

# Ramp
path_ramp = 'Kankberg_Data/ramp.tif'
ds_ramp = rasterio.open(path_ramp)
ramp = ds_ramp.read(1)

# Observation wells for Model 3
path_obs = 'Kankberg_Data/obswell_M3.tif'
ds_obs = rasterio.open(path_obs)
obs = ds_obs.read(1)

# Recharge in UM1988 area
path_RUM1988 = 'Kankberg_Data/recharge_M2.tif'
ds_RUM1988 = rasterio.open(path_RUM1988)
RUM1988 = ds_RUM1988.read(1)

# Recharge in UM2012 area
path_RUM2012 = 'Kankberg_Data/recharge_M3.tif'
ds_RUM2012 = rasterio.open(path_RUM2012)
RUM2012 = ds_RUM2012.read(1)
```

Plot rasters

In [3]:
```
# Areas for boundaries - peat och outofbounds

fig = plt.figure(figsize=(10, 5))
gs = gridspec.GridSpec(1, 2, width_ratios=[1, 1])
fig.suptitle("Micellanious", fontsize=16)


masked_peat = (peat == 1) # Create a masked array where nodata values are masked
transform = ds_peat.transform
xmin, ymin = transform * (0, 0)
xmax, ymax = transform * (masked_peat.shape[1], masked_peat.shape[0])

ax1 = plt.subplot(gs[0])
im1 = ax1.imshow(masked_peat, extent=[xmin, xmax, ymin, ymax])
cbar = plt.colorbar(ax1.imshow(masked_peat, cmap='viridis', interpolation='nearest'), ax=ax1)
cbar.ax.set_ylabel('true/false')
ax1.set_xlabel('Longitude')
ax1.set_ylabel('Latitude')
ax1.set_title('Peat')


#No flow
transform = ds_noflow.transform                          # access the affine transformation
xmin, ymin = transform * (0, 0)                          # (col, row) för en nollpunkt
xmax, ymax = transform * (noflow.shape[1], noflow.shape[0])

ax2 = plt.subplot(gs[1])
im2 = ax2.imshow(noflow, extent=[xmin, xmax, ymin, ymax])
cbar = plt.colorbar(ax2.imshow(noflow, cmap='viridis', interpolation='nearest'), ax=ax2)
cbar.ax.set_ylabel('true/false')
ax2.set_xlabel('Longitude')
ax2.set_ylabel('Latitude')
ax2.set_title('no flow')

plt.tight_layout()
plt.show()
```

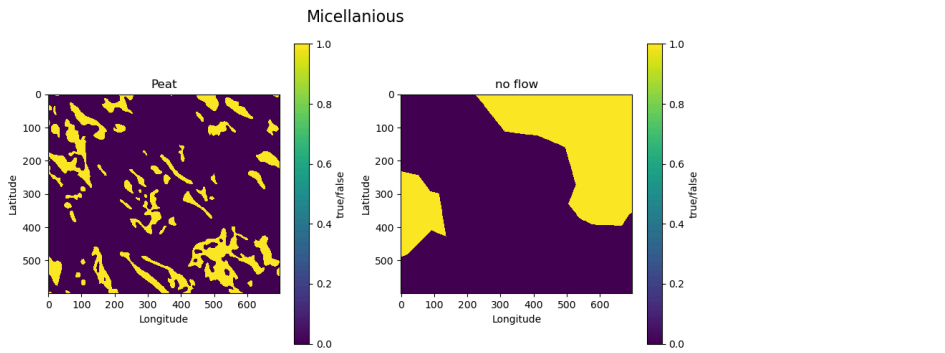

In [4]:
```
# lakes and rivers
fig = plt.figure(figsize=(10, 5))
gs = gridspec.GridSpec(1, 2, width_ratios=[1, 1])
fig.suptitle("Watercourses in the area of interest", fontsize=16)

#lakes
lakes=lake
lakes = np.where(lakes == 4, 0, lakes)
lakes = np.where(lakes == 5, 0, lakes)

transform = ds_lake.transform
xmin, ymin = transform * (0, 0)
xmax, ymax = transform * (lakes.shape[1], lakes.shape[0])

ax1 = plt.subplot(gs[0])
cmap = plt.cm.YlGnBu
im = plt.imshow((lakes>0), cmap=cmap, extent=[xmin, xmax, ymin, ymax], interpolation='none')
plt.colorbar()
ax1.set_xlabel('Longitude')
ax1.set_ylabel('Latitude')
ax1.set_title('Lakes')


#rivers
rivers = river
rivers = np.where(noflow == 1, 0, rivers)
rivers = np.where(lake == 4, 1, rivers)
rivers = np.where(lake == 5, 1, rivers)

transform = ds_river.transform
xmin, ymin = transform * (0, 0)
xmax, ymax = transform * (rivers.shape[1], rivers.shape[0])

ax2 = plt.subplot(gs[1])
cmap = plt.cm.YlGnBu
im = plt.imshow(rivers, cmap=cmap, extent=[xmin, xmax, ymin, ymax], interpolation='none')
cbar = plt.colorbar(im, ax=ax2)
cbar.ax.set_ylabel('true/false')
ax2.set_xlabel('Longitude')
ax2.set_ylabel('Latitude')
ax2.set_title('Rivers')

plt.show()
```

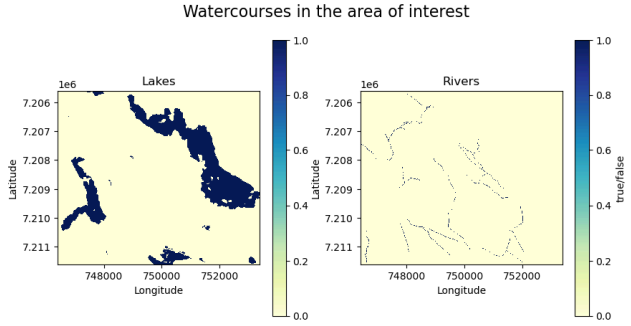

In [5]:
```
# Create a figure and gridspec layout
fig = plt.figure(figsize=(10, 5))
gs = gridspec.GridSpec(1, 2, width_ratios=[1, 1])
fig.suptitle("Topographical information 10x10 resolution", fontsize=16)

#Topography, defined with the CH lakes
new_top = top
new_top = np.where(lakes > 20, lakes, top)        # Making sure topography is aligned with the lakes
new_top = np.where(lakes == 2, 217.5, new_top)    # Klocktråsket
new_top = np.where(lakes == 3, 220, new_top)      # Gillervattnet
new_top = np.where(lakes == 10, 195.5, new_top)   # Innersttjärnet
new_top = np.where(lakes == 12, 212, new_top)     # Avatjärnet

new_top = np.where(lakes == 11, 219, new_top)     # Part of Gillervattnet, not CH-cells, but modified topography

transform = ds_top.transform
xmin, ymin = transform * (0, 0)
xmax, ymax = transform * (new_top.shape[1], new_top.shape[0])

ax1 = plt.subplot(gs[0])
im1 = ax1.imshow(new_top, extent=[xmin, xmax, ymin, ymax])
cbar = plt.colorbar(ax1.imshow(new_top, cmap='viridis', interpolation='nearest'), ax=ax1)
cbar.ax.set_ylabel('Elevation (m)')
```

```
ax1.set_xlabel('Longitude')
ax1.set_ylabel('Latitude')
ax1.set_title('Topography')


#Bedrock
nodata_value = ds_bed.nodata
new_bed_nd = np.where(bed == nodata_value, new_top, bed)            # Replace nodata values with a new value (e.g., 0),
th = 3                                                              # Threshold value (m)
d_top_bed = new_top - new_bed_nd                                    # delta top - bed
new_bed = np.where(d_top_bed < th, (new_top-th), new_bed_nd)        # Replace the "negative depths" with bed=top

transform = ds_bed.transform
xmin, ymin = transform * (0, 0)
xmax, ymax = transform * (new_bed.shape[1], new_bed.shape[0])

ax2 = plt.subplot(gs[1])
im2 = ax2.imshow(new_bed, extent=[xmin, xmax, ymin, ymax])
#cbar = plt.colorbar(im2, ax2=ax2)
cbar = plt.colorbar(ax2.imshow(new_bed, cmap='viridis', interpolation='nearest'), ax=ax2)
cbar.ax.set_ylabel('Elevation (m)')
ax2.set_xlabel('Longitude')
ax2.set_ylabel('Latitude')
ax2.set_title('Bedrock')

plt.tight_layout()
plt.show()
```

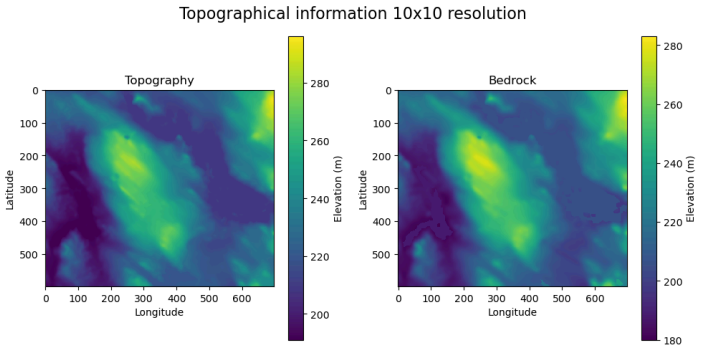

Model set-up

In [6]:
```
modelname = 'Model3_1'
exe_name='Exe/MODFLOW-NWT_64.exe'   # Where we stored our executable files
model_ws='Results_M3_1'             # The model will run in the folder Results_M3_1
```

In [7]:
```
# Model workspace package
mf = flopy.modflow.Modflow(modelname, exe_name=exe_name, version='mfnwt', model_ws=model_ws)
```

In [8]:
```
# Solver package for MODFLOW-NWT-64 bit executable file
nwt = flopy.modflow.ModflowNwt(mf, headtol=0.0001, maxiterout=100, linmeth=2)
```

Discretization

In [9]:
```
# x,y grid discretization
nrow = new_top.shape[0]      # number of rows
ncol = new_top.shape[1]      # number of columns
Lx = int(xmax-xmin)          # total dimension in x, coordinates
Ly = int(ymin-ymax)          # total dimension in y, coordinates
delr = Lx/ncol               # resolution of cell grid, spacing for rows and columns.
delc = Ly/nrow               # Should be the same resolution as the raster files.
```

In [10]:
```
# z/layer discretization
ztop = new_top                                          # top elevation, in m.a.s.l.
nlay = 7                                                # number of layers
gn = 281.03                                             # "Gruvnollan", reference point for the local system

# bottom of layers
zbot0 = new_bed                                         # soil, layer 0
zbot1 = (new_bed-50)                                    # bedrock, layer 1
zbot2 = (new_bed-100)                                   # bedrock, layer 2
zbot3 = gn-320.                                         # bedrock, layer 3, the bottom of UM1988 & top of UM2012
zbot4 = gn-530.                                         # bedrock, layer 4, the bottom of UM2012
zbot5 = gn-1000.                                        # bedrock, layer 5, the bottom of expansion, UM20XX
zbot6 = gn-1500.                                        # depth of the model. Also in m.a.s.l.

zbot = [zbot0, zbot1, zbot2, zbot3, zbot4, zbot5, zbot6]    # array with bottom of all layers, last one is bottom of model
```

In [11]:
```
# Calculate layer thickness for conductance, later
lay0 = ztop - zbot0
lay0 = np.average(lay0)
lay1 = zbot0 - zbot1
lay1 = np.average(lay1)
lay2 = zbot1 - zbot2
lay2 = np.average(lay2)
lay3 = zbot2 - zbot3
lay3 = np.average(lay3)
lay4 = zbot3 - zbot4
lay5 = zbot4 - zbot5
lay6 = zbot5 - zbot6

layth = [lay0, lay1, lay2, lay3, lay4, lay5, lay6]
```

In [12]:
```
# Discretization object package
dis = flopy.modflow.ModflowDis(mf, nlay, nrow, ncol, delr=delr, delc=delc, top=ztop, botm=zbot)
```

Boundaries

Defining boundary grids by geospatial processing

In [13]:
```
# Defining lake areas
lake_cells2d = (lakes > 20)
```

```
lake2 = (lakes == 2)
lake3 = (lakes == 3)
lake10 = (lakes == 10)
lake12 = (lakes == 12)

lake_cells3d = np.tile(lake_cells2d[np.newaxis, :, :], (nlay, 1, 1))
lake2_3d = np.tile(lake2[np.newaxis, :, :], (nlay, 1, 1))
lake3_3d = np.tile(lake3[np.newaxis, :, :], (nlay, 1, 1))
lake10_3d = np.tile(lake10[np.newaxis, :, :], (nlay, 1, 1))
lake12_3d = np.tile(lake12[np.newaxis, :, :], (nlay, 1, 1))

# Defining noflow areas in edges
noflow_cells2d = (noflow == 1)
noflow_cells3d = np.tile(noflow_cells2d[np.newaxis, :, :], (nlay, 1, 1))

# Defining peat areas
peat_cells2d = (masked_peat == True)

# Defining river cells
river_cells2d = (rivers > 0)

# Defining the range for south boundary
south = range(40, 210)

# Defining the range for north boundary
north = range(0, 120)

# Defining the range for east boundary
east = range(530, 540)
```

Boundaries

In [14]:
```
# 3D boundary grid
ibound = np.ones((nlay, nrow, ncol), dtype=np.int32)  # active cells in the whole matrix

ibound[:, 0, north] = -1                              # constant head boundary northwest corner,
ibound[:, -1, south] = -1                             # constant head boundary southwest corner
ibound[:, east, -1] = -1                              # constant head boundary southeast corner

ibound[noflow_cells3d] = 0                            # noflow on "edges"

ibound[lake_cells3d] = -1                             # constant head in Bastuträsket, Stavträsket
ibound[lake2_3d] = -1                                 # constant head in Klockträsket
ibound[lake3_3d] = -1                                 # constant head in Gillervattnet
ibound[lake10_3d] = -1                                # constant head in Innersttjärnet
ibound[lake12_3d] = -1                                # constant head in Avatjärnet
```

In [15]:
```
# Plot boundaries

cmap = plt.cm.YlGnBu
plt.imshow(ibound[0,:,:], cmap=cmap, interpolation='none')
plt.colorbar()
plt.title("Boundaries", fontsize=16)
plt.show()
```

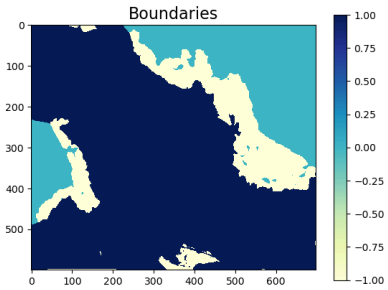

Initial levels

In [16]:
```
# Initial groundwater levels grid

strt = np.zeros((nrow, ncol), dtype=np.float32)
strt = np.where(peat_cells2d == True, new_top, new_top)    # Initial levels
strt = np.where(lake_cells2d == True, new_top, strt)       # Initial level in lakes

strt[-1, south] = 195                                      # South CH boundary
strt[0, north] = 217.5                                     # Klockträsket boundary
strt[east, -1] = 226.5                                     # East CH boundary, Småmyrorna
```

In [17]:
```
# Bas package for boundaries and starting levels
bas = flopy.modflow.ModflowBas(mf, ibound=ibound, strt=strt)
```

Recharge

In [18]:
```
# Defining recharge

R0 = 0                  # m/day, no recharge (lakes, rivers, peat)
R1 = 180/(1000*365)     # normal recharge (soil)
R2 = 100/(1000*365)     # low recharge (slope areas)
R3 = 320/(1000*365)     # higher recharge in UM1988 area of influence
R4 = 220/(1000*365)     # higher recharge in UM2012 area of influence

# Matrix with normal recharge
rech = np.ones((nrow, ncol), dtype=np.float32)*R1
rech = np.where(slope > 5, R2, rech)              # Lower recharge in steep areas, higher than 5%
rech = np.where(peat == True, R0, rech)           # No recharge in peat areas, regular recharge elsewhere
rech = np.where(lakes > 0, R0, rech)              # No recharge in lakes
rech = np.where(rivers > 0, R0, rech)             # No recharge in rivers
rech = np.where(noflow == 1, R0, rech)            # No recharge in noflow areas
rech = np.where(RUM2012 == True, R4, rech)        # Higher recharge in mine areas
rech = np.where(RUM1988 == True, R3, rech)        # Higher recharge in mine areas
```

In [19]:
```
# Plot recharge
cmap = plt.cm.YlGnBu
plt.imshow(rech, cmap=cmap, interpolation='none')
plt.colorbar()
plt.title("Recharge", fontsize=16)
plt.show()
```

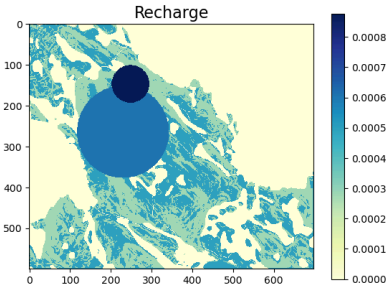

In [20]:
```
# Recharge package
rch = flopy.modflow.ModflowRch(mf, nrchop=3, rech=rech)
```

Parameters/properties

Hydraulic conductivity

In [21]:
```
# Defining hydraulic conductivity

# Soil, layer0. Morän.
hk0 = 9.6*(10**(-6))     # horizontal hydraulic conductivity, m/s
hk0 = hk0*86400          # hk, m/d is default.

# Bedrock, layer1.
hk1 = 3*(10**(-7))
hk1 = hk1*86400

# Bedrock, layer2.
hk2 = 9*(10**(-8))
hk2 = hk2*86400

# Bedrock, layer3.
hk3 = 9*(10**(-8))
hk3 = hk3*86400

# Bedrock, layer4.
hk4 = 9*(10**(-9))
hk4 = hk4*86400

# Bedrock, layer5.
hk5 = 8*(10**(-9))
hk5 = hk5*86400

# Bedrock, layer6.
hk6 = 8*(10**(-10))
hk6 = hk6*86400

# "Total" hydraulic conductivity
hk = [hk0, hk1, hk2, hk3, hk4, hk5, hk6]
vka = [1,1,1,1,1,1,1] # defined as a factor of hk. Connected to layvka=[1,1,1,1,1,1,1].
```

In [22]:
```
# Add UPW package to add hydraulic conductivity
upw = flopy.modflow.ModflowUpw(mf, laytyp=[1,0,0,0,0,0,0], hk=hk, vka=vka, layvka=[1,1,1,1,1,1,1], ipakcb=53)
```

Rivers

Removing RIV cells

In [23]:
```
# Removing RIV cells very close to CH cells
ibound2d = ibound[0,:,:]

ch_riv = np.zeros((nrow, ncol), dtype=np.float32)

for i in range(rivers.shape[0]):
    for j in range(rivers.shape[1]):
        if rivers[i,j] > 0:

            # If a RIV cell is side by side a CH cell, double layers of non-functioning RIV cells.
            if (i > 0 and ibound2d[i-1,j] == -1) or \
              (i < rivers.shape[0]-1 and ibound2d[i+1,j] == -1) or \
              (j > 0 and ibound2d[i,j-1] == -1) or \
              (j < rivers.shape[1]-1 and ibound2d[i,j+1] == -1) or \
              (i > 0 and ibound2d[i-2,j] == -1) or \
              (i < rivers.shape[0]-2 and ibound2d[i+2,j] == -1) or \
              (j > 0 and ibound2d[i,j-2] == -1) or \
              (j < rivers.shape[1]-2 and ibound2d[i,j+2] == -1) or \
              (i > 0 and ibound2d[i-3,j] == -1) or \
              (i < rivers.shape[0]-3 and ibound2d[i+3,j] == -1) or \
              (j > 0 and ibound2d[i,j-3] == -1) or \
              (j < rivers.shape[1]-3 and ibound2d[i,j+3] == -1):

              ch_riv[i,j] = True
```

In [24]:
```
# Removing RIV cells because of the soil depth
soildepth = new_top-new_bed

sd_riv = np.zeros((nrow, ncol), dtype=np.float32)

for i in range(rivers.shape[0]):
    for j in range(rivers.shape[1]):
        if rivers[i,j] > 0:
            if soildepth[i,j] < 4:

                sd_riv[i,j] = True
```

Defining rivers

In [25]:
```
# Defining RIV cells

list = []
for i in range(rivers.shape[0]):
    for q in range(rivers.shape[1]):
        if rivers[i,q] > 0:
            if ch_riv[i,q] == False:
                if sd_riv[i,q] == False:
                    if soildepth[i,q] < 6:
                        list.append([0, i, q, new_top[i,q]-3.9, 1, (new_top[i,q]-4)])     # layer, row, column, elevation, conductance, rbot
```

```
                else:
                    list.append([0, i, q, new_top[i,q]-5.9, 1, (new_top[i,q]-6)])     # layer, row, column, elevation, conductance, rbot
river_spd = {0:list}
```

In [26]:
```
# river package to include the streams
riv = flopy.modflow.ModflowRiv(mf, stress_period_data=river_spd)
```

Draining structures

In [27]:
```
fig = plt.figure(figsize=(10, 5))
gs = gridspec.GridSpec(1, 2, width_ratios=[1, 1])
fig.suptitle("Topographical information 10x10 resolution", fontsize=16)

# Underground mines, UM1988 & UM2012
transform = ds_um.transform
xmin, ymin = transform * (0, 0)
xmax, ymax = transform * (um.shape[1], um.shape[0])

ax1 = plt.subplot(gs[0])
im1 = ax1.imshow(um, extent=[xmin, xmax, ymin, ymax])
plt.plot(248, 145, marker='X', markersize=1, markerfacecolor='blue') # rätt plottat med raderna som y-axel och kolumnerna som x-axel

cbar = plt.colorbar(ax1.imshow(um, cmap='YlGnBu', interpolation='nearest'), ax=ax1)
cbar.ax.set_ylabel('Current mine')
ax1.set_xlabel('Longitude')
ax1.set_ylabel('Latitude')
ax1.set_title('Current mine')


# Ventilation shafts
transform = ds_vs.transform
xmin, ymin = transform * (0, 0)
xmax, ymax = transform * (vs.shape[1], vs.shape[0])

ax2 = plt.subplot(gs[1])
im2 = ax2.imshow(vs, extent=[xmin, xmax, ymin, ymax])
cbar = plt.colorbar(ax2.imshow(vs, cmap='YlGnBu', interpolation='nearest'), ax=ax2)
cbar.ax.set_ylabel('Elevation (m)')
ax2.set_xlabel('Longitude')
ax2.set_ylabel('Latitude')
ax2.set_title('Ventilation shafts')


plt.tight_layout()
plt.show()
```

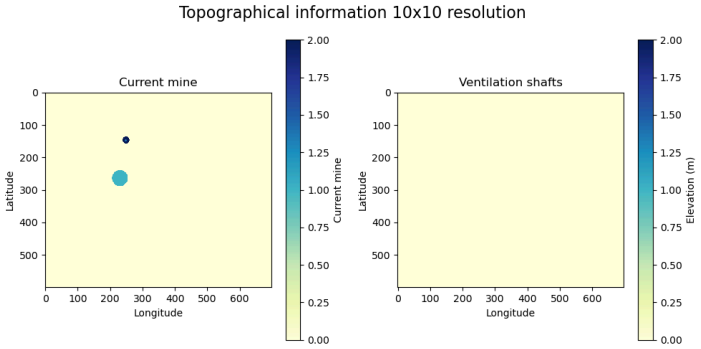

In [28]:
```
# Sediment Thickness in Drn cell
st = np.ones((nrow, ncol), dtype=np.float32)*0.1
st_ramp = 5

# Layer thickness averages depending on the mine location
UM2012 = (um == 1)
UM1988 = (um == 2)

# 1988 Underground mine (UM1988) layer thickness averages
UM1988_layth = np.zeros((nrow, ncol), dtype=np.float32)

for r in [0, 1, 2, 3]:
    for i in range(um.shape[0]):
        for q in range(um.shape[1]):
            if UM1988[i,q] == 1:
                UM1988_layth[i,q] = np.average(layth[r])

# Ramp layer thickness averages
ramp_layth =  np.zeros((nrow, ncol), dtype=np.float32)

for r in [3, 4]:
    for i in range(um.shape[0]):
        for q in range(um.shape[1]):
            if ramp[i,q] == 1:
                ramp_layth = np.average(layth[r])

# Ventilation shafts layer thickness averages
vs_layth =  np.zeros((nrow, ncol), dtype=np.float32)

for r in [0, 1, 2, 3, 4]:
    for i in range(um.shape[0]):
        for q in range(um.shape[1]):
            if vs[i,q] == 1:
                vs_layth = np.average(layth[r])
```

Conductance

In [29]:
```
# Hydraulic conductivity for calibration with varying K, m3/s.
hk0c = hk0
hk1c = hk1
hk2c = hk2
hk3c = hk3
hk4c = hk4
hk5c = hk5
hk6c = hk6
hk_c = [hk0c, hk1c, hk2c, hk3c, hk4c, hk5c, hk6c]  # m3/day
```

In [30]:
```
# Sediment Thickness in Drn cell
st = np.ones((nrow, ncol), dtype=np.float32)*0.1
st_ramp = 5

# Areas for UM1988 Drn cells
A0 = (layth[0]-st)*delr      # Average values of layer thickness in layer0-3
A1 = (layth[1]-st)*delr
A2 = (layth[2]-st)*delr
A3 = (layth[3]-st)*delr
A4 = (layth[4]-st)*delr
A5 = (layth[5]-st)*delr
A6 = (layth[6]-st)*delr

A = [A0, A1, A2, A3, A4, A5, A6]

# Area for ramp Drn cells
A_ramp1 = (layth[3]-st_ramp)*delr
A_ramp2 = 5*delr

# Delta L
L = delc

# Conductance for mines according to Darcy's
C0 = hk_c[0]*A[0]/L
C1 = hk_c[1]*A[1]/L
C2 = hk_c[2]*A[2]/L
C3 = hk_c[3]*A[3]/L
C4 = hk_c[4]*A[4]/L
C5 = hk_c[5]*A[5]/L
C6 = hk_c[6]*A[6]/L

C = [C0, C1, C2, C3, C4, C5, C6]

# Conductance for ramp
C3r = (hk3*A_ramp1/L)
C4r = (hk4*A_ramp2/L)
```

In [31]:
```
# 3d matrix of zbot
zbot3d = np.ones((nlay, nrow, ncol), dtype=np.float32)
for r in [0, 1, 2, 3, 4, 5, 6]:
    zbot3d[r,:,:] = zbot[r]

# 3d matrix for the conductances
C3d = np.ones((nlay, nrow, ncol), dtype=np.float32)
for r in [0, 1, 2, 3, 4, 5, 6]:
    C3d[r,:,:] = C[r]
```

Defining drain cells

In [32]:
```
st = 0.1
list = []

# Conductance factors for calibration
condfact_vs = np.ones((nlay, nrow, ncol), dtype=np.float32) * 1
condfact_UM2012 = np.ones((nlay, nrow, ncol), dtype=np.float32) * 1

# 2012 Underground mine (UM2012)
for i in range(um.shape[0]):
    for q in range(um.shape[1]):
        if um[i,q] == 1:
            list.append([4, i, q, zbot4+st, C3d[r, i, q]*condfact_UM2012[r, i, q]])

# Ventilation shafts
for r in [0, 1, 2, 3, 4]:
    for i in range(um.shape[0]):
        for q in range(um.shape[1]):
            if vs[i,q] == 1:
                list.append([r, i, q, (zbot3d[r, i, q]+st), C3d[r, i, q]*condfact_vs[r, i, q]])

spd_drn = {0:list}
```

Additional code to model the ramp & expansion UM20XX # Ramp - 2 depths for i in range(um.shape[0]): for q in range(um.shape[1]): if ramp[i,q] == 1: list.append([3, i, q, (zbot3d[2, i, q]-5), C3r*condfact_ramp[3, i, q]]) elif ramp[i,q] == 2: list.append([4, i, q, (zbot3d[3, i, q]-5), C4r*condfact_ramp[4, i, q]]) # 20XX Expanded underground mine (UM20XX) for i in range(um.shape[0]): for q in range(um.shape[1]): if um[i,q] == 1: list.append([5, i, q, zbot5+st, C3d[r, i, q]])

In [33]:
```
# Drain package
drn = flopy.modflow.ModflowDrn(mf, stress_period_data=spd_drn)
```

UM1988/well

In [34]:
```
# Define the pumping rate, here equal to the measured inflow
Q_UM1988 = -(15.7+2.5/2) * 24  # m3/d

# Define the location of the well
UM1988_layer = 3
UM1988_row = 145
UM1988_col = 248

# 1988 Underground mine (UM1988) stress period data
well_data = [UM1988_layer, UM1988_row, UM1988_col, Q_UM1988]

# Define the stress period data dictionary
spd_wel = {0: [well_data]}
```

In [35]:
```
# Create the well package
wel = flopy.modflow.ModflowWel(mf, stress_period_data=spd_wel)
```

Model solver

In [36]:
```
# Add OC package for output control

spd = {(0, 0): ['save head', 'print budget', 'save budget']}
oc = flopy.modflow.ModflowOc(mf, stress_period_data=spd, compact=True)
```

In [37]:
```
# Write the MODFLOW input files
mf.write_input()
```

In [38]:
```
#Run the MODFLOW model
mf.run_model()
```

```
FloPy is using the following executable to run the model: ..\Exe\MODFLOW-NWT_64.exe

                                MODFLOW-NWT-SWR1
    U.S. GEOLOGICAL SURVEY MODULAR FINITE-DIFFERENCE GROUNDWATER-FLOW MODEL
                             WITH NEWTON FORMULATION
                             Version 1.3.0 07/01/2022
                        BASED ON MODFLOW-2005 Version 1.12.0 02/03/2017

                        SWR1 Version 1.05.0 03/10/2022

 Using NAME file: Model3_1.nam
 Run start date and time (yyyy/mm/dd hh:mm:ss): 2024/06/07 17:21:08

 Solving:  Stress period:     1    Time step:     1    Groundwater-Flow Eqn.
 Run end date and time (yyyy/mm/dd hh:mm:ss): 2024/06/07 17:25:20
 Elapsed run time:  4 Minutes, 12.321 Seconds

  Normal termination of simulation
```

Out[38]: (True, [])

Results

In [39]:
```
# Positions for cross sections

UM1988 = 147  # centered
UM2012 = 265  # centered
ramp1 = 158   # 158-197
ramp2 = 198   # 198-240
VS1 = 243
VS2 = 268
VS3 = 287
```

In [40]:
```
# Extract heads
hds = bf.HeadFile(model_ws+'/'+modelname+'.hds')
times = hds.get_times()                          #timesteps
head = hds.get_data(totim = times[-1])           #head from last timestep
```

In [41]:
```
# Plotting the heads
masked_head = np.ma.masked_where(head == np.min(head) , head) # Create a masked array where nodata values are masked

plt.figure(figsize=(10, 8))
plt.imshow(masked_head[1, :, :], cmap='viridis', extent=(0, head.shape[2], head.shape[1], 0))
plt.colorbar(label='Head')
plt.title('Head Distribution')
plt.xlabel('Column')
plt.ylabel('Row')
plt.show()
```

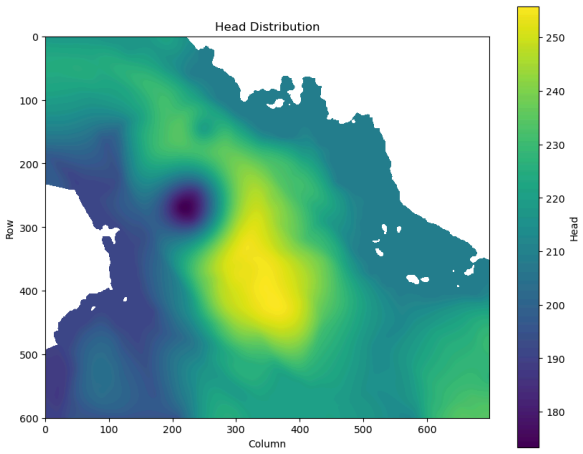

Observation wells & heads comparison

In [42]:
```
# Observation wells locations
obsKA0501 = (obs == 501)
obsKA0502 = (obs == 502)
obsKA0503 = (obs == 503)
obsKA0505 = (obs == 505)
obs1 = (obs == 1)          # Norra Åkulla, old "Well 1"
obs2 = (obs == 2)          # Södra Åkulla, old "Well 2"

# New observation wells
obsKA2103B = (obs == 2103)
obsKA2104B = (obs == 2104)
obsKA2106B = (obs == 2106)
obs3 = (obs == 10)         # Västra Åkulla
```

In [43]:
```
# Observation wells reference values

obsref = np.zeros((nrow, ncol), dtype=np.float32)
obsref = np.where(obsKA0501 == True, 236.2, obsref)      # KA0501
obsref = np.where(obsKA0502 == True, 213.4, obsref)      # KA0502
obsref = np.where(obsKA0503 == True, 233, obsref)        # KA0503, KA0504 (mean value)
obsref = np.where(obsKA0505 == True, 227, obsref)        # KA0505, soil well

obsref = np.where(obs1 == True, 207.2, obsref)           # Norra Åkulla
obsref = np.where(obs2 == True, 221, obsref)             # Södra Åkulla


# Additional observation wells
obsref = np.where(obsKA2103B == True, 211.1, obsref)     # KA2103B
obsref = np.where(obsKA2104B == True, 203.3, obsref)     # KA2104B
obsref = np.where(obsKA2106B == True, 179.9, obsref)     # KA2106B
obsref = np.where(obs3 == True, 201, obsref)             # Västra Åkulla

obsref3d = np.tile(obsref[np.newaxis, :, :], (nlay, 1, 1))
```

In [44]:
```
# Heads at obs wells compared to field measurements.

hds_obs = np.zeros((nlay, nrow, ncol), dtype=np.float32)

for r in [0, 1]:
    for i in range(obs.shape[0]):
        for q in range(obs.shape[1]):
            if obs[i,q] != 0:
                hds_obs[r, i, q] = masked_head[r, i, q]
```

In [45]:
```
# Comparison of modelled hds & field measurements at observation wells

comp = (hds_obs - obsref3d) # Difference in m between hds_obs & obsref.

wel_location = [((np.where(obsKA0501 == True)), 'KA0501'),
                ((np.where(obsKA0502 == True)), 'KA0502'),
                ((np.where(obsKA0503 == True)), 'KA0503'),
                ((np.where(obsKA0505 == True)), 'KA0505'),
                ((np.where(obs1 == True)), 'Norra Åkulla'),
                ((np.where(obs2 == True)), 'Södra Åkulla'),

                # Additional wells
                ((np.where(obsKA2103B == True)), 'KA2103B'),
                ((np.where(obsKA2104B == True)), 'KA2104B'),
                ((np.where(obsKA2106B == True)), 'KA2106B'),
                ((np.where(obs3 == True)), 'Västra Åkulla')]

comp_val = []
for r in [0, 1]:
    for wloc in wel_location:
        indices, name = wloc
        row, col = indices
        comp_val.append((r, name, comp[r, row, col]))

for rlay in [0]:
    print()
    for r, name, value in comp_val:
        if r == rlay:
            print(f"{name}: {value}")
        if name == 'Södra Åkulla':
            print()
        if name == 'KA0505':
            print()
```

```
KA0501: [-3.136612]
KA0502: [10.82843]
KA0503: [-9.759186]
KA0505: [-6.0028534]

Norra Åkulla: [9.782883]
Södra Åkulla: [-7.505234]

KA2103B: [6.019928]
KA2104B: [-10.324722]
KA2106B: [2.9445648]
Västra Åkulla: [1.3744812]
```

RSME plot & calculation

In [46]:
```
obs_arr = [obsKA0501,  obsKA0502, obsKA0503, obsKA0505, obs1, obs2, obsKA2103B, obsKA2104B, obsKA2106B, obs3]
obs_arr_label = ['KA0501', 'KA0502','KA0503', 'KA0505', 'Norra Åkulla', 'Södra Åkulla', 'KA2103B', 'KA2104B', 'KA2106B', 'Västra Åkulla']


for r, label in zip(obs_arr, obs_arr_label):
    plt.scatter(hds_obs[0, r], obsref3d[0, r], label=label)

# Add line representing the 45-degree line
plt.plot([0, 300], [0, 300], color='red', linestyle='--')

# Set labels and title
plt.xlabel('Model heads (m)')
plt.ylabel('Observed heads (m)')
plt.legend()

# Show plot
plt.grid(True)
plt.axis('equal')  # Set equal aspect ratio

plt.show()
```

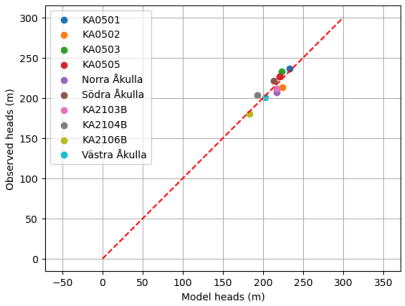

In [47]:
```
errors = np.array([item[2][0] for item in comp_val])

# Calculate squared errors
squared_errors = (errors) ** 2

# Calculate mean squared error
mean_squared_error = np.mean(squared_errors)

# Calculate RMSE
rmse = np.sqrt(mean_squared_error)

print("RMSE:", rmse)
```

```
RMSE: 7.5616016
```

Plot cross sections

In [48]:
```
# Read out the CellBudgetFile (binary cell by cell flow file)
cbb = bf.CellBudgetFile(model_ws + '/' + modelname + '.cbc') # code to extract the values of the file
kstpkper_list = cbb.get_kstpkper()

frf = cbb.get_data(text="FLOW RIGHT FACE", totim=times[-1])[0] # capital letters bc thats how it is written in output file
fff = cbb.get_data(text="FLOW FRONT FACE", totim=times[-1])[0]
flf = cbb.get_data(text="FLOW LOWER FACE", totim=times[-1])[0]
```

In [50]:
```
# Plot UM2012

# extent
xmin = 1500
xmax = 3000
zmin = -300
zmax = np.max(ztop)

fig = plt.figure(figsize=(14, 5))
ax = fig.add_subplot(1, 1, 1)
xsect = flopy.plot.PlotCrossSection(model=mf, line={'Row':UM2012}, extent=(xmin, xmax, zmin, zmax))
linecollection = xsect.plot_grid(color='lightgrey')
plt.title('2012 Underground mine (UM2012)')

# Boundaries
patches = xsect.plot_ibound(head=head)

# Plot water table
wt_colors = ['blue', 'red', 'green', 'cyan', 'magenta', 'lightgrey']
for i, color in enumerate(wt_colors):
    if i < head.shape[0]:
        wt = xsect.plot_surface(head[i], masked_values=[999.], color=color, lw=0.5)

# Plot flow direction
#vectors = xsect.plot_vector(frf, fff, flf)

plt.plot(2710,  obsref[obsKA2103B], marker='o', markersize=2, markerfacecolor='blue')    # col x-axel, depth som y-axel
plt.text(2710,  obsref[obsKA2103B], 'KA2103', fontsize=8, ha='center', va='bottom')      # 2103: row 249, col 271

plt.plot(2010, obsref[obsKA2106B], marker='o', markersize=2, markerfacecolor='blue')
plt.text(2010, obsref[obsKA2106B], 'KA2106', fontsize=8, ha='center', va='bottom')       # 2106: row 261, col 201

plt.plot(2041, obsref[obsKA2104B], marker='o', markersize=2, markerfacecolor='blue')
plt.text(2041, obsref[obsKA2104B], 'KA2104', fontsize=8, ha='center', va='bottom')       # 2104.0: row 290, col 241

plt.plot(2410, obsref[obs3], marker='o', markersize=2, markerfacecolor='blue')
plt.text(2410, obsref[obs3], 'Västra Åkulla', fontsize=8, ha='center', va='bottom')      # Västra Åkulla: row 312, col 182

plt.plot(2130, obsref[obs1], marker='o', markersize=2, markerfacecolor='blue')
plt.text(2130, obsref[obs1], 'Norra Åkulla', fontsize=8, ha='center', va='bottom')       # Norra Åkulla: row 213, col 194
```

Out[50]:
```
Text(2130, [207.2], 'Norra Åkulla')
```

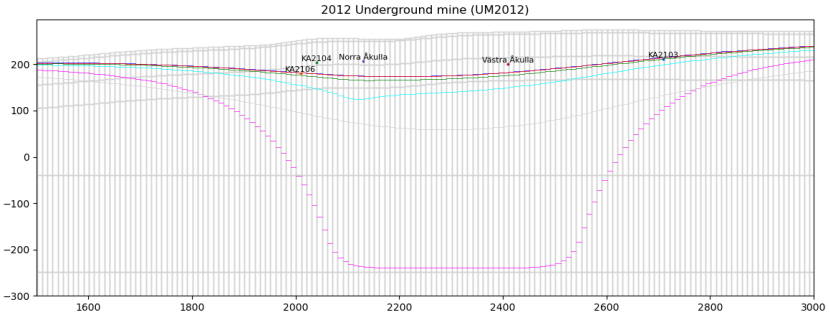

In [52]:
```
# Plot UM1988

# Extent
xmin = 2000
xmax = 3000
zmin = -200
zmax = np.max(ztop)

fig = plt.figure(figsize=(14, 5))
ax = fig.add_subplot(1, 1, 1)
xsect = flopy.plot.PlotCrossSection(model=mf, line={'Row':159}, extent=(xmin, xmax, zmin, zmax))
plt.title('1988 Underground mine (UM1988)')
linecollection = xsect.plot_grid(color='lightgrey')

# Boundaries
patches = xsect.plot_ibound(head=head)

# Plot water tables
wt = xsect.plot_surface(head[0], masked_values=[999.], color='blue', lw=0.5)
wt = xsect.plot_surface(head[1], masked_values=[999.], color='red', lw=0.5)
wt = xsect.plot_surface(head[3], masked_values=[999.], color='green', lw=0.5)
wt = xsect.plot_surface(head[4], masked_values=[999.], color='cyan', lw=0.5)
wt = xsect.plot_surface(head[5], masked_values=[999.], color='magenta', lw=0.5)

plt.plot(2240, obsref[obsKA0501], marker='o', markersize=2, markerfacecolor='blue') # col x-axel, depth som y-axel
plt.text(2240,  obsref[obsKA0501], '501', fontsize=8, ha='center', va='bottom')      # 0501.0: row 159, col 224

plt.plot(2400, obsref[obsKA0503], marker='o', markersize=2, markerfacecolor='blue')  # col x-axel, depth som y-axel
plt.text(2400, obsref[obsKA0503], '502', fontsize=8, ha='center', va='bottom')     # 502.0: row 139, col 240

plt.plot(2760, obsref[obsKA0503], marker='o', markersize=2, markerfacecolor='blue')  # col x-axel, depth som y-axel
plt.text(2760, obsref[obsKA0503], '503', fontsize=8, ha='center', va='bottom')     # 0503.0: row 127, col 276

plt.plot(2810, obsref[obsKA0505], marker='o', markersize=2, markerfacecolor='blue')  # col x-axel, depth som y-axel
plt.text(2810, obsref[obsKA0505], '505', fontsize=8, ha='center', va='bottom')       # 0505.0: row 124, col 281

plt.show()
```

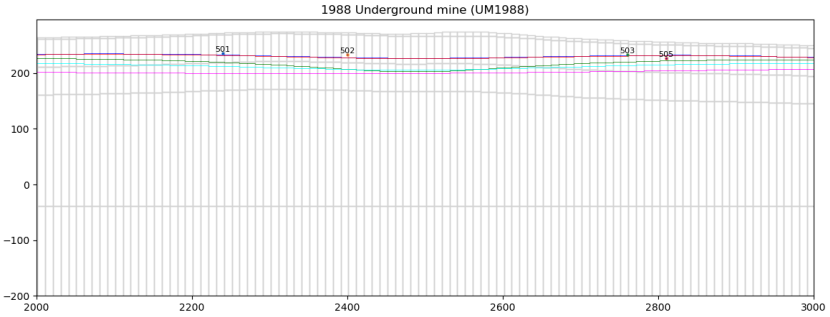

Plot area of interest

In [53]:
```
#Plot the area of influence.
#The area of influence could be adjusted to fit to the wanted comparison

fig = plt.figure(figsize=(20, 20))
ax = fig.add_subplot(1, 1, 1, aspect="equal")
modelmap = flopy.plot.PlotMapView(model=mf, layer=0, ax=ax)
qm = modelmap.plot_ibound()
plt.title('Area of influence')

cmin = 0.3            # The criteria for being an area of influence (drawdown = 0.3m)
cmax = np.max(head)   # High amount of influence
cnum = 25             # number of contour lines

# Heads from where ever you want to compare the modelled results with
M1_0hds = bf.HeadFile('Results_M1_0/Model1_0.hds')
times = M1_0hds.get_times()                    #timesteps
M1_0head = M1_0hds.get_data(totim = times[-1])          #head from last timestep
M1_0head = np.ma.masked_where(head == np.min(M1_0head), M1_0head) # Create a masked array where nodata values are masked

# Choose drawdown comparison (change M1_0head)
drawdown = (M1_0head-masked_head[0,:,:])

cs = modelmap.contour_array(drawdown, levels=np.linspace(cmin, cmax, cnum), linestyles=['--' if level != cmin else '--' for level in np.linspace(cmin, cmax, cnum)])
plt.clabel(cs, inline=1, fontsize=15, fmt="%1.2f")

plt.show()
```

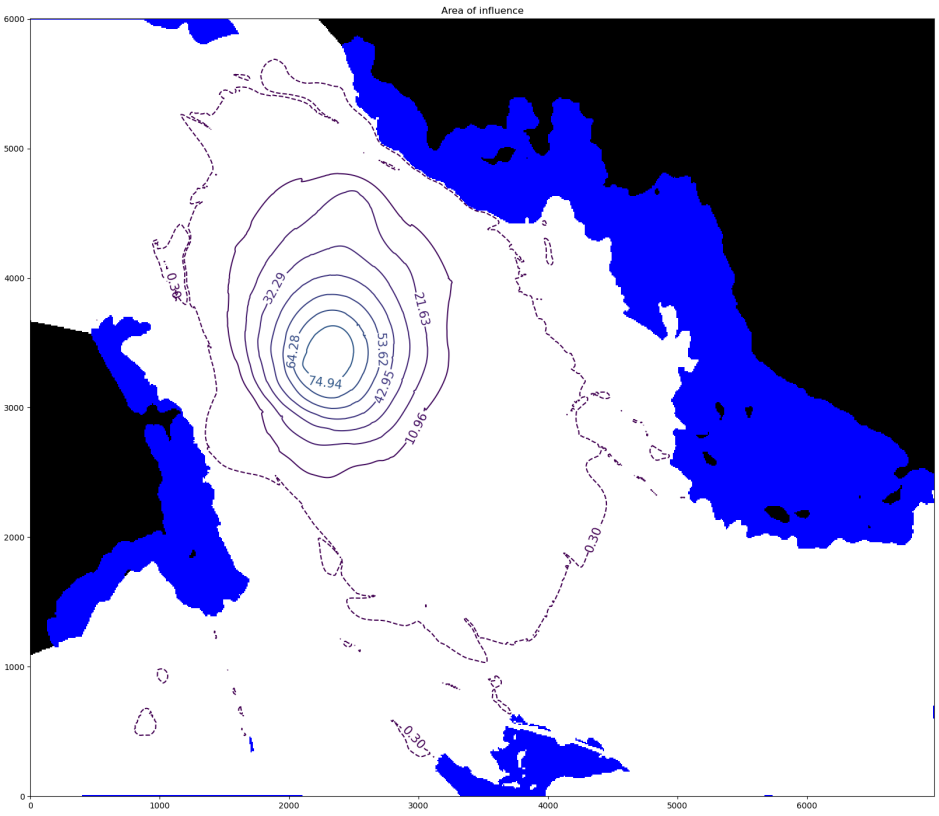

DEPARTMENT OF ARCHITECTURE AND CIVIL ENGINEERING
CHALMERS UNIVERSITY OF TECHNOLOGY
Gothenburg, Sweden
www.chalmers.se

CHALMERS
UNIVERSITY OF TECHNOLOGY